Reassessing southern African silcrete geochemistry: Implications for silcrete origin and sourcing of silcrete artefacts

John A. Webb[1†] and David J. Nash[2,3]

[1] Department of Ecology, Environment and Evolution, La Trobe University, Bundoora, Victoria 3086, Australia.

[2] School of Environment and Technology, University of Brighton, Lewes Road, Brighton, BN2 4GJ, United Kingdom.

[3] School of Geography, Archaeology and Environmental Studies, University of the Witwatersrand, Johannesburg, South Africa

[†]corresponding author: john.webb@latrobe.edu.au

ABSTRACT:

A synthesis of the geochemistry of silcretes and their host sediments in the Kalahari Desert and Cape coastal zone, using isocon comparisons, shows that silcretes in the two regions are very different. Kalahari Desert silcretes outcrop along drainage-lines and within pans, and formed by groundwater silicification of near-surface Kalahari Group sands. Silicification was approximately isovolumetric. Few elements were lost; Si and K were gained as microquartz precipitated in the sediment porosity and glauconite formed in the suboxic groundwater conditions. The low Ti content reflects the composition of the host sands. Additional elements in the Kalahari Desert silcretes were supplied in river water and derived from weathering of silicates in basement rocks. Evaporation under an arid climate produced high-pH groundwater that mobilised and precipitated Si; this process is still occurring.

In the Cape coastal zone, pedogenic silcretes cap hills and plateaus, overlying deeply weathered argillaceous bedrock. Silicification resulted from intensive weathering that destroyed the bedrock silicates, almost completely removing most elements and causing a substantial volume decrease. Some of the silica released formed a microcrystalline quartz matrix, and most Ti precipitated as anatase, so the Cape silcretes contain relatively high Ti levels. The intense weathering that formed the Cape silcretes could have occurred in the Eocene, during and after the Palaeocene-Eocene Thermal Maximum, when more acidic rainfall and high temperatures resulted in intensified silicate weathering world-wide. This could have been responsible for widespread formation of pedogenic silcretes elsewhere in Africa and around the globe.

Trace element sourcing of silcrete artefacts to particular outcrops has most potential in the Cape, where differences between separate bedrock areas are reflected in the silcrete composition. In the Kalahari Desert, gains of some elements can override compositional differences of the parent material, and sourcing should be based on elements that show the least change during silicification.

KEYWORDS: silcrete, South Africa, Kalahari Desert, isocon, artefact sourcing

1. Introduction

After Australia, southern Africa contains the most extensive coverage of silcrete (silica-cemented duricrust) in the world (Figure 1). Silcrete occurs in two distinct geographical and sedimentological contexts. In the centre of the subcontinent, silcretes occur within Kalahari Group sediments, with outcrops described from the presently arid to semi-arid Kalahari Desert (e.g. Summerfield, 1982; 1983c; Nash et al., 1994b; Nash et al., 1994a; Nash and Shaw, 1998; Shaw and Nash, 1998; Nash et al., 2004; Ringrose et al., 2005; Ringrose et al., 2009; Nash et al., 2013a; Ringrose et al., 2014; Nash et al., 2016) and the tropical southern Congo Basin (e.g. Veatch, 1935; Cahen and Lepersonne, 1952; Linol et al., 2015; Linol et al., 2019). In the more temperate Cape coastal zone of South Africa, silcretes largely occur capping dissected plateaus developed on deeply weathered bedrock (Frankel and Kent, 1938; Bosazza, 1939; Frankel, 1952; Mountain, 1952; Summerfield, 1981; 1983c; b; Nash et al., 2013b).

Whilst much has been written about southern African silcretes, it remains unclear why silica-cemented duricrusts have developed in two such different geological and geomorphological contexts. Summerfield (1983a) proposed that silcretes in the Kalahari Desert developed in alkaline, semi-arid environments, whilst the majority of Cape coastal silcretes formed under more humid tropical, low-pH conditions; this is primarily because the latter contain pedogenic structures and overlie deeply weathered profiles, both lacking in Kalahari Desert silcretes.

Other inferences about silcrete genesis in the Kalahari Desert and Cape coastal zone have been made on the basis of geochemical data. Cape coastal silcretes have a higher Ti content than their Kalahari Desert counterparts, so Summerfield (1983a) postulated that higher Ti 'weathering profile silcretes' indicated hot, humid palaeoenvironments at the time of silicification, whilst Ti-poor 'non-weathering profile silcretes' reflected more arid environments. However, it has been shown that Ti levels are more closely related to parent material chemistry than palaeoclimate (Milnes and Twidale, 1983; Young, 1985; Twidale and Hutton, 1986; Nash et al., 1994a; Webb and Golding, 1998).

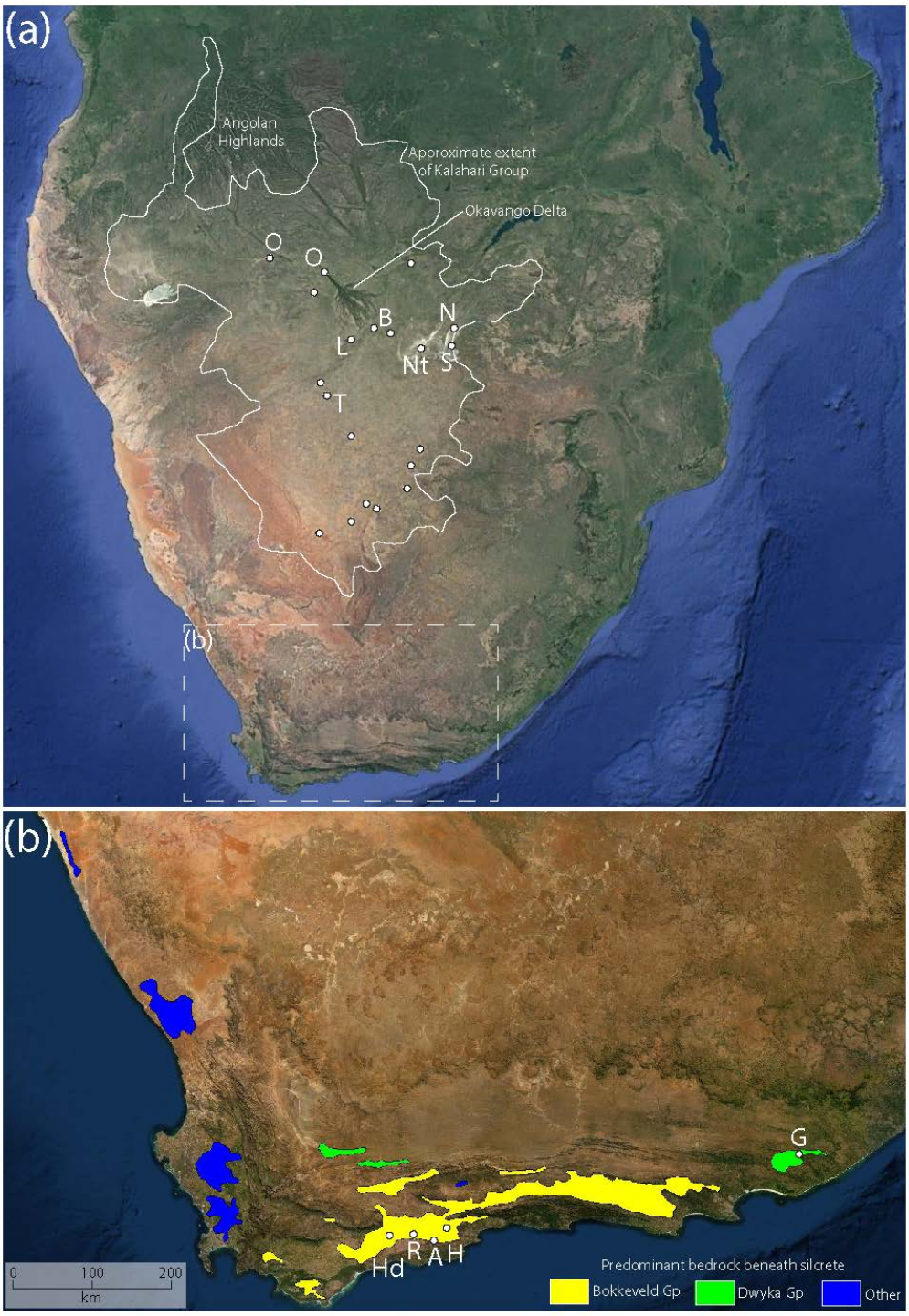

Figure 1
Distribution of silcrete in the Kalahari Desert and Cape coastal zone. Distribution of Cape silcretes is generalised from Roberts (2003); note that the actual area of silcrete occupies only a small proportion of the shaded areas. Kalahari Desert silcrete localities are shown as dots. Localities of analysed samples are shown as follows. Okavango system: O – Okavango River, L – Lake Ngami, B – Boteti River, S – Sua Pan, N – Nata River, Nt – Ntwetwe Pan; outside Okavango system: T - Tswaane. Cape: A – Albertinia, R – Riversdale, H – Herbertsdale, Hd – Heidelberg, G – Grahamstown. (a) Google Earth image downloaded January 7, 2020, ©DigitalGlobe. (b) World View satellite image (obtained January 7, 2020 through Global Mapper).

Silcretes from different parts of the Kalahari Desert and Cape coastal zone have different trace element compositions (Nash et al., 2013a; Nash et al., 2013b). This has been used to identify likely source areas for artefacts from Middle Stone Age archaeological sites in the Kalahari Desert (Nash et al., 2013a; Nash et al., 2016). However, the geochemical basis of this differentiation is unclear, in particular whether it represents differences in the material hosting the silcrete or the silicification mechanism itself. Nash et al. (2013a) suggested from their studies in the Kalahari Desert that differences in host sediment composition were critical, but this has yet to be rigorously tested. Furthermore, uncertainties remain in terms of the magnitude of the compositional differences needed to definitively indicate different sources.

This paper presents the first meta-analysis of the substantial number of published geochemical analyses of silcrete and host bedrock/sediments now available for southern Africa. It aims to (i) identify more precisely the constraints on and timing of silcrete formation and (ii) determine the robustness of silcrete artefact sourcing investigations in the subcontinent. The study focusses on silcrete genesis in the Kalahari Desert and Cape coastal zone only. Silcretes are present elsewhere in southern Africa, e.g in the Congo Basin (Linol et al., 2019), but limited chemical data for selected elements are available for these silcretes, so they could not form part of this geochemical study.

2. Silcretes in the Cape coastal zone and Kalahari Desert

Silcretes outcrop extensively along the southern Cape coastal zone of South Africa (Figure 1), where they occur along drainage lines or, most commonly, as subhorizontal caprocks on partially dissected plateaus which represent palaeosurfaces (e.g. around Grahamstown; Figure 2a); isolated outcrops in a particular area frequently lie at the same level (Summerfield, 1981; Roberts, 2003). Cape silcretes almost exclusively overlie deeply weathered saprolite (Figures 2b, c) developed upon argillaceous bedrock, most commonly either Late Carboniferous to Early Permian Dwyka Group or Lower Devonian Bokkeveld Group. Other host rocks in particular areas include Mesoproterozoic granites and gneisses, Neoproterozoic metasediments and Early Jurassic dolerites; in addition, silicified Cenozoic sediments may form the upper part of some silcrete profiles (Roberts, 2003).

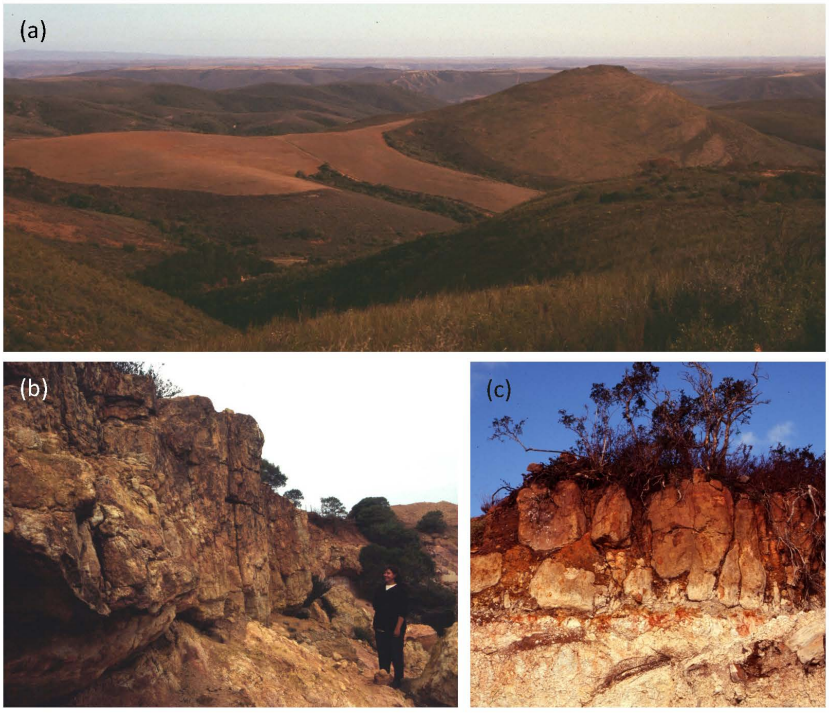

Figure 2
Silcretes in the Cape coastal zone: (a) View of a silcrete-capped palaeosurface near Grahamstown; (b) 2.5 m thick pedogenic silcrete profile at Rooikop, east of Grahamstown; (c) 2.3 m thick pedogenic silcrete profile developed above red mottled and bleached weathered bedrock, Enniskillin, near Grahamstown.

Cape coastal silcretes are of variable thickness, typically 1-3 m but exceeding 8 m in some locations (Mountain, 1952; Roberts, 2003). Most have pronounced vertical to sub-vertical jointing, giving a columnar appearance (Figure 2c) (Summerfield, 1983c). Both massive and glaebular silcretes are common, and glaebular horizons may overlie brecciated layers that grade into massive silcrete (Frankel and Kent, 1938; Summerfield, 1981). All of these features are suggestive of formation by pedogenic silicification (cf. Thiry and Milnes, 1991; Thiry, 1999; Nash and Ullyott, 2007; Ullyott and Nash, 2016; Thiry and Milnes, 2017).

Silcretes occur within the surface and near-surface sediments of the Kalahari Group (e.g. Nash et al., 1994b; Linol et al., 2015), which comprises several different formations mostly deposited in aeolian, fluvial and lacustrine environments (Du Plessis, 1993; Haddon and McCarthy, 2005). The surface sediments, which have undergone aeolian transport in many areas, comprise predominantly red-orange, well-sorted, fine to medium grained, quartz-rich unconsolidated sand, interbedded with clayey and silty sands (Milzow et al., 2009). The

Kalahari sands represent the world's largest body of sand, covering over 2.5 million km^2 of central and southern Africa (Figure 1) (Thomas and Shaw, 1991).

The majority of Kalahari Desert silcrete outcrops occur in, or close to, landscape depressions (Figures 3a, b) such as pans and fossil valley systems (Summerfield, 1982; Shaw and de Vries, 1988; Nash et al., 1994b; Nash et al., 1994a; Shaw and Nash, 1998; Nash et al., 2004; Ringrose et al., 2005; Kampunzu et al., 2007) where the surface aeolian, fluvial and lacustrine sediments have been cemented (Summerfield, 1982). They include the only examples of silcrete in the world considered to be forming at the present day (MacGregor, 1931; Shaw et al., 1990). Surface silcrete occurrences are usually localised and vary from gravel lags on the margins of pans (Summerfield, 1982; Nash and Shaw, 1998) to irregular or lenticular layers up to 7 m thick in the flanks of valleys and as part of palaeolake shorelines (Figure 3) (Shaw and de Vries, 1988; Nash et al., 1994a; Ringrose et al., 2005; Kampunzu et al., 2007; Ringrose et al., 2009). The silcretes are typically massive (Figures 3b, c) and lack pedogenic structures, suggesting that they formed by groundwater silicification at or near the watertable (Nash et al., 1998; Ullyott et al., 1998; Nash and Ullyott, 2007; Ullyott and Nash, 2016). Partial or complete replacement of pre-existing calcrete is widespread, and silcretes may also rarely be associated with ferricretes (e.g. Nash et al., 1994b; Nash et al., 1994a; Nash and Shaw, 1998; Nash et al., 2004; Ringrose et al., 2005).

Most Kalahari Desert silcretes consist of quartz grains inherited from the parent sands lying within chalcedonic silica and/or microquartz cements (Summerfield, 1982). Void fills are common and are composed of a variety of silica polymorphs: α-quartz, opal-CT or opal-T, and moganite (e.g. Summerfield, 1982; Nash et al., 1994b; Nash and Hopkinson, 2004).

3. Data sources and methodology

3.1. Geochemical data sources

To understand the processes by which silcretes in the Kalahari and Cape have formed, it is necessary to compare the chemical composition and mineralogy of the host bedrock/ sediment and the silcrete developed within or upon this bedrock/sediment. There is a large amount of analytical data available for both the host lithologies and the silcretes that outcrop either within or directly above these lithologies, so no new data were collected for this study.

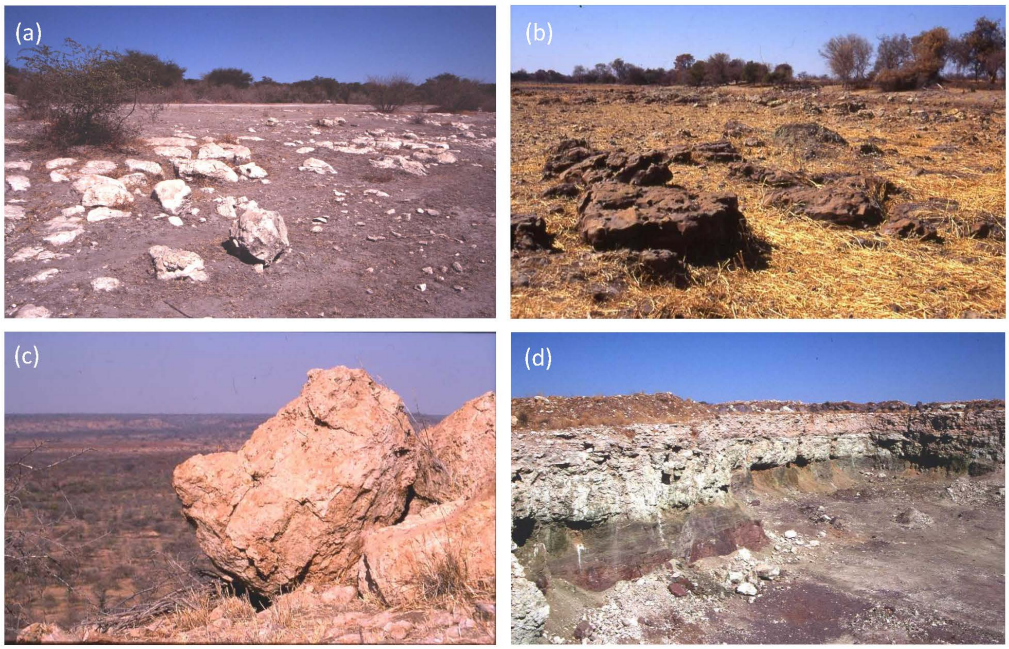

Figure 3
Silcretes in the Kalahari Desert: (a) Localised silcrete outcrop in the floor and flanks of the Xaudum Valley, northwest Botswana; (b) Drainage-line silcrete in the floor of the Boteti River at Samedupe, north-central Botswana; (c) Silcrete exposed in an escarpment at the eastern edge of the Kalahari Group sediments, Sesase, Botswana; (d) Complex 5 m thick silcrete-calcrete profile overlying granitoid-gneiss bedrock at Tswaane Quarry, central Botswana.

For the Cape silcretes, analyses of Dwyka or Bokkeveld Group bedrock and associated silcretes were compiled from a number of sources: Dwyka Group - 25/23 major/trace element analyses (Frankel and Kent, 1938; Summerfield, 1983b; Huber et al., 2001); Bokkeveld Group - 50/47 major/trace element analyses (Summerfield, 1983b; Marker et al., 2002; Fourie, 2010); silcretes developed on Dwyka Group - 18/13 major/trace element analyses (Frankel and Kent, 1938; Summerfield, 1983b; Nash et al., 2013b); silcretes developed on Bokkeveld Group - 81/29 major/trace element analyses (Bosazza, 1939; Frankel, 1952; Summerfield, 1983b; Nash et al., 2013b). Few, if any, bedrock and silcrete analyses are available for other host rocks for the Cape silcretes, so this study is restricted to understanding silcrete development on Dwyka and Bokkeveld Group bedrock only. Sample localities of both silcretes and bedrock are scattered across the entire area of silcrete and bedrock outcrop, and the analyses are therefore believed to be representative of the

composition of these rock types. Only analyses of fresh or relatively fresh bedrock were included in this study. Summerfield (1984) analysed silcrete and underlying heavily weathered or altered bedrock at three locations in the Cape. However, because fresh bedrock was not analysed, his bedrock data are not used here.

For the Kalahari Desert, the chemical composition and mineralogy of silcretes and host sediments within the endorheic Okavango system in the Middle Kalahari were compared. Both sediments and silcretes in this region have been extensively studied and analysed: sands - 180/37 major/trace element analyses (McCarthy and Metcalfe, 1990; McCarthy et al., 1991; McCarthy and Ellery, 1995; Huntsman-Mapila et al., 2005); silcretes - 82/78 major/trace element analyses (Summerfield, 1982; Nash and Shaw, 1998; Nash et al., 2013a). Only sediments and silcretes in areas directly affected by the Okavango River and/or Delta and its outflows (either present-day or past) were considered; these included analyses from sites along river channels, within lake basins and pans, and within the Okavango Delta itself. Additional major and trace element data are available for silcretes within valleys directed towards the Okavango Delta (e.g. the Xaudum; Nash et al., 2013a) and Makgadikgadi Basin (e.g. the Okwa; Nash et al., 2004); however, there are no analyses of unsilicified sediments associated with these silcretes, so they were not considered further.

All available analytical data for silcretes in the Kalahari Desert were used to calculate the overall median composition of Kalahari silcrete: 134/86 major/trace element analyses (Summerfield, 1982; Nash et al., 1994a; Nash and Shaw, 1998; Nash et al., 2004; Nash et al., 2013a). This was then compared with the analyses from the Okavango Delta system (as defined above) to determine if the Okavango sediments and silcretes are broadly representative of those in the Kalahari Desert as a whole.

Geochemical data acquired through both X-ray fluorescence (XRF) and inductively coupled plasma mass spectrometry (ICP-MS) were included within this study; as will be discussed, the fact that consistent results were obtained using disparate data sets gives more confidence to the findings. It should be noted that not all analyses contained the same number of elements, so the number of analyses for each element varies; the numbers given above are a maximum.

3.2. Geochemical data analysis

In this study, a detailed geochemical analysis was carried out using isocon plots (Grant, 2005), whereby concentrations of components in an altered rock (e.g. silcrete) are plotted against those in the parent material. The isocon plots were compiled using median elemental contents of silcretes and their parent lithologies, in order to obtain the overall chemical trends accompanying silicification. For one silcrete outcrop (close to Grahamstown in the Cape coastal zone; Frankel and Kent, 1938), analyses of parent material immediately underlying a silcrete were available, so this isocon could be compared with the isocons obtained using median analyses. Complete element analyses were not available for all data sets, so some isocons lack particular elements.

In these plots, the isocon is a straight line from the origin passing through points for all components that are immobile (i.e. showing no enrichment or depletion relative to the parent). In silcrete studies, Zr is selected as the immobile element (Webb and Golding, 1998; Nash et al., 2004), because it is present as zircon, which is one of the least soluble minerals (Thornber, 1992) and is extremely resistant to weathering and diagenetic processes (Pettijohn, 1941; Morton, 1984). Angular to well-rounded fragments of zircon are common in silcretes and exhibit sharp, unaltered boundaries with no evidence of etching (Watts, 1978; Webb and Golding, 1998; Eggleton and Taylor, 2017).

On isocon plots, elements that fall above or below the isocon have been respectively enriched or depleted in the altered material (in this case silcrete) plotted on the vertical axis. The gain or loss of mobile elements during silicification can be calculated as a percentage of the parent composition:

$$\%\ gain\ loss = \frac{\left(C_{silcrete} \times \frac{Zr_{parent}}{Zr_{silcrete}}\right) - C_{parent}}{C_{parent}} \times 100 \qquad \text{Equation 1}$$

where C is the concentration of a particular element.

The volume change during silicification can be calculated from the Zr content and densities of the silcrete and parent material:

$$\frac{V_{parent}}{V_{silcrete}} = \frac{Zr_{silcrete}}{Zr_{parent}} \times \frac{density_{silcrete}}{density_{parent}} \qquad \text{Equation 2}$$

If silcrete formation occurred at constant volume, as shown by the preservation of original textures from the parent material, then the ratio of the Zr contents is the inverse of the density ratio.

The results of our analyses are now discussed thematically, first for the Cape coastal zone (section 4) and then for the Kalahari Desert (section 5).

4. Cape silcretes

4.1. Composition and mineralogy of the Dwyka and Bokkeveld Group bedrock

The Bokkeveld Group is composed largely of mudstones with minor sandstones; the mudstones are black when fresh and consist of quartz, illite, some chlorite (clinochlore) and feldspars (albite, orthoclase, microcline) (Fourie, 2010). Zircon is the most abundant heavy mineral; brookite, rutile and monazite also occur. Available geochemical data show that the median chemical composition of Bokkeveld Group mudstones (Table 1) is dominated by SiO_2 and Al_2O_3 due to the quartz and clay content. The strong correlation of Al_2O_3 with K_2O ($r^2 = 0.95$) reflects the dominance of illite as the Al-bearing mineral in these rocks. The Al_2O_3 and K_2O concentrations are very strongly correlated with Ba, Rb, Cs, Sc and Ga, implying that all these trace elements are present in illite. The substantial amount of Fe_2O_3 (7%) probably occurs as iron oxides. There is too much TiO_2 (1%) for it to exist entirely as brookite/rutile; probably most is present in clays.

In comparison, the Dwyka Group consists largely of diamictites, which contain clasts of quartz, feldspar (plagioclase, K-feldspar) and rock fragments in a clay matrix (kaolinite, smectite, illite); there may be minor amounts of pyroxene, chlorite and carbonate (calcite and minor dolomite), along with trace levels of opaque minerals (mainly magnetite, minor sulfides), epidote, garnet, muscovite, biotite, zircon and amphibole (Reimold et al., 1997; Huber et al., 2001). The different mineralogy of the Dwyka Group compared to the Bokkeveld Group means that, although the composition is also dominated by SiO_2 and Al_2O_3, the Dwyka Group contains greater levels of Na_2O, CaO and MgO (Table 1), reflecting the higher percentage of plagioclase and Mg silicates (both as individual grains and as a component of igneous rock fragments). There is no significant correlation between Al_2O_3 and K_2O or most trace elements because there are a number of different Al-bearing minerals present. K_2O is strongly correlated with Rb because these elements will readily substitute for each other in K-bearing minerals. The Fe_2O_3 concentrations are strongly correlated ($r^2 = 0.81$-0.82) with Mn and LOI, suggesting that Fe is mainly present as ferric oxide/hydroxide minerals that contain significant levels of Mn. As for the Bokkeveld Group, the TiO_2 present probably occurs mostly in clays.

4.2. Composition and mineralogy of the Cape silcretes

Cape coastal zone silcretes consist predominantly of quartz as floating inherited quartz grains in a matrix of microquartz (Summerfield, 1981; 1983c; b). In addition, there is a significant amount of microcrystalline anatase, often as alternating lamellae of silica and anatase in geopetal concave-upwards colloform structures (Frankel and Kent, 1938; Summerfield, 1983c; b).

Available geochemical data show that there is little difference in the composition of silcretes developed on Dwyka Group or Bokkeveld Group strata (apart from three elements, discussed below), so they are considered together. Overall, the median composition of the Cape silcretes (Table 1) is dominated by SiO_2 (95%) with small amounts of TiO_2 (1.7%), Fe_2O_3 (0.9%) and Al_2O_3 (0.5%) and very low levels (<0.05%) of all other major elements, including MgO, CaO, Na_2O and K_2O. The trace element present in the highest concentrations is Zr (~500 ppm); there are moderate levels (>10 ppm) of Ba, Nb, Sr, Pb, Hf, Y, Cu and Ce (in decreasing order of abundance), and low levels (<5 ppm) of other trace elements. The only difference between silcretes developed on Dwyka Group or Bokkeveld Group strata is that the latter silcretes contain significantly smaller amounts of Fe_2O_3, Cr and V.

The TiO_2 content of Cape silcrete primarily reflects the presence of anatase (although trace amounts of the Ti-bearing heavy minerals brookite/rutile may also be present). TiO_2 concentrations in the silcretes are very strongly correlated (r^2>0.98) with Nb and Ta; the close similarity in ionic radius between Ti, Nb and Ta means that anatase can contain substantial amounts of Nb and Ta (Huy et al., 2012). TiO_2 is also strongly correlated (r^2 = 0.8-0.94) with many heavy rare earth elements (HREEs; Er, Ho, Lu, Tm, Y, Yb) as well as a number of other trace elements (Sn, U, W, Co, Mo), suggesting that the anatase in the silcretes contains these elements as well.

Zr is probably present as zircon, because Zr concentrations are very strongly correlated (r^2 = 0.99) with those of Hf, and zircon often contains minor amounts of Hf (Wang et al., 2010). Fe_2O_3 is present as iron oxides; the strong correlation of Fe_2O_3 with Cr, V, As, Se and Te (r^2 = 0.72-0.81) indicates that these trace elements occur within the iron oxides. The higher level of Fe_2O_3 in the Dwyka Group silcretes is reflected in their greater Cr and V concentrations.

4.3. Formation of the Cape silcretes

Isocon comparisons were made between the median compositions of Dwyka and Bokkeveld Group sediments and the respective overlying silcretes (Table 2; Figure 4). In addition, a comparison was made using Frankel and Kent's (1938) analyses of silcrete and directly underlying Dwyka Group bedrock at Grahamstown; only major element analyses are available in their study, so median Zr concentrations from Dwyka Group sediments and silcrete were used to construct this isocon.

All three isocons are very similar (Figure 4) and show almost complete loss of most major elements during silicification (Al_2O_3, Fe_2O_3, CaO, MgO, Na_2O, K_2O and LOI; mostly >90%), together with some loss of SiO_2 and TiO_2 (40-60%). Most trace elements are also lost; Hf, Ta and Nb show the lowest losses (<50%). The fact that three independent sets of data show the same results strongly suggests that the same silicification process has been active for all Cape silcretes encompassed by the available analyses.

To calculate the volume change during silicification using Equation 2, it is necessary to know the density of the parent bedrock and the overlying silcrete. The density of Dwyka Group sediments has been measured as 2.46-2.58 g/cc (Bothma, 2015). No density data are available for the Bokkeveld Group, but the values are likely to be very similar to those of shales in the Ecca Group (2.53-2.76 g/cc; Baiyegunhi et al., 2019), given the similarity in lithology. The density of the Cape silcretes, based on their porosity (~2%; Schmidt et al., 2017) and anatase content (~2%) is ~2.62. Inserting these values into Equation 2 along with the median Zr concentrations of silcrete and bedrock, the ratio of volume of parent bedrock : volume of silcrete is 2.5-2.8 for the Bokkeveld Group silcretes and 3.5-3.9 for the Dwyka Group silcretes (Table 2). Thus, there has been a substantial volume loss during formation of the Cape silcretes; a 3 m thick silcrete (typical maximum thickness; Roberts, 2003) represents an original bedrock thickness of 7.5-12 m. This loss in volume matches the almost complete loss of most major and trace elements evident from the isocon analysis.

In contrast to this finding, Summerfield (1984) regarded formation of the Cape silcretes as isovolumetric. This suggestion was based on Mountain's (1952) record of intensively leached Dwyka diamictite retaining undistorted ghosts of the boulders occurring in the subjacent fresh bedrock, and thin sub-vertical quartz veins that continue without disruption from fresh Bokkeveld Group bedrock into overlying deeply weathered material. However, neither of these observations referred directly to the silcretes, and the consistency of the isocon results, obtained from separate stratigraphic units using different analytical techniques (XRF and

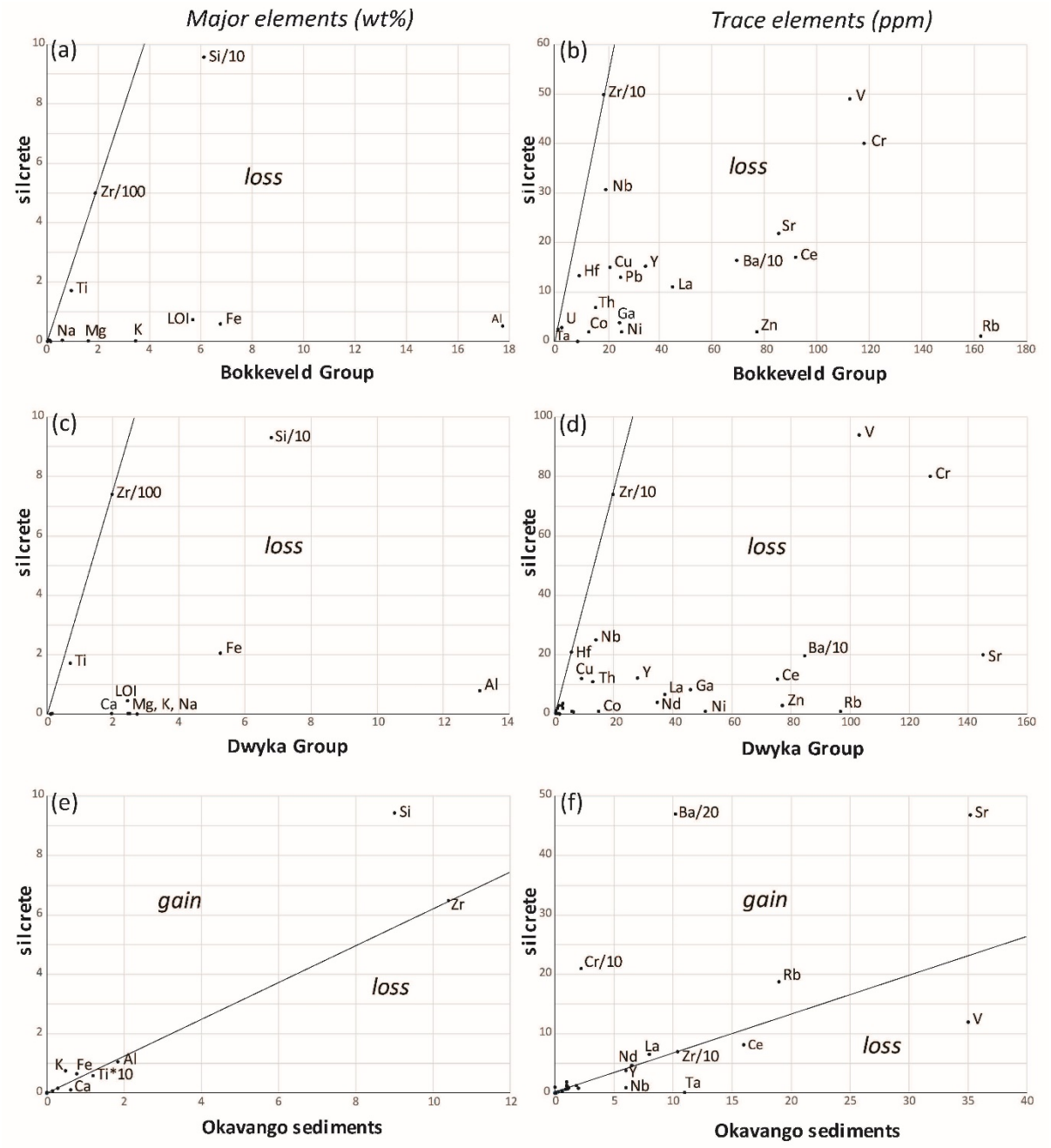

Figure 4
Major and trace element isocon plots for: (a, b) Bokkeveld Group bedrock and associated silcretes (c, d) Dwyka Group Group bedrock and associated silcretes (e, f) Okavango delta sediments and associated silcretes. See Figure 1 for locations of silcrete samples, Table 1 for data.

ICP-MS) run at different laboratories, substantiates the fact that that substantial volume loss occurred. Roberts (2003) illustrated Cape silcretes with intact cross-stratification that haveformed within Cenozoic sediments. However, these are groundwater silcretes that have undergone isovolumetric silicification; they show none of the features (columnar jointing, glaebular horizons overlying brecciated layers) typical of the pedogenic silcretes developed

on the Bokkeveld and Dwyka Group strata. No analyses are available for the groundwater silcretes or their host sediments, so they were not included in the isocon analysis.

Silicification of the Cape silcretes was accompanied by retention of the detrital quartz component (as shown by textural analysis; Summerfield, 1983b; a). Clays and any other silicate minerals in the clay-rich host lithologies were broken down during silcrete formation, and most of the constituent elements completely removed from the system (Figures 5a, b), apart from much of the silica (retained as a microcrystalline quartz matrix) and the TiO_2 (largely retained as neoformed anatase). The silcretes overlying Dwyka and Bokkeveld Group rocks contain more TiO_2 (1.7%) than the parent rocks (0.7-1%), even though some Ti is lost during silicification, because of the substantial volume reduction demonstrated by the isocons.

As Si, Ti and the other elements were released by weathering (Figures 5a, b), they moved vertically downwards through the profile in infiltrating rainwater, most likely during alternating phases of wetting and drying accompanying pedogenesis (cf. Thiry and Milnes, 1991; Thiry and Simon-Coinçon, 1996; Thiry, 1999). The gravitational movement of solutions during silicification is clearly indicated by the vertically stacked concave-upwards colloform structures in the Cape silcretes, composed of alternating lamellae of silica and anatase (Frankel and Kent, 1938).

Three trace elements (apart from Zr) show the lowest losses during silicification: Nb, Ta and Hf. Most of the Nb and Ta was incorporated into anatase as it formed; as discussed above, anatase often contains significant levels of Nb and Ta. Hf was retained within zircon, because this mineral is unaffected by weathering and silicification. Hf and Zr are strongly correlated within the silcretes but not the parent strata, probably because Hf in the Bokkeveld and Dwyka Group sediments is present in both clays and zircon; only that in zircon was retained during silicification.

Only a small percentage of most trace elements was retained during silicification; in the silcretes, many of these elements are correlated with TiO_2 or Fe_2O_3 (as discussed above), suggesting that formation of anatase and retention of some iron oxide resulted in the associated preservation of a large suite of trace elements, albeit at low levels. The role of anatase is not surprising as nanocrystalline anatase has been shown to adsorb contaminant metals (Kanna et al., 2005).

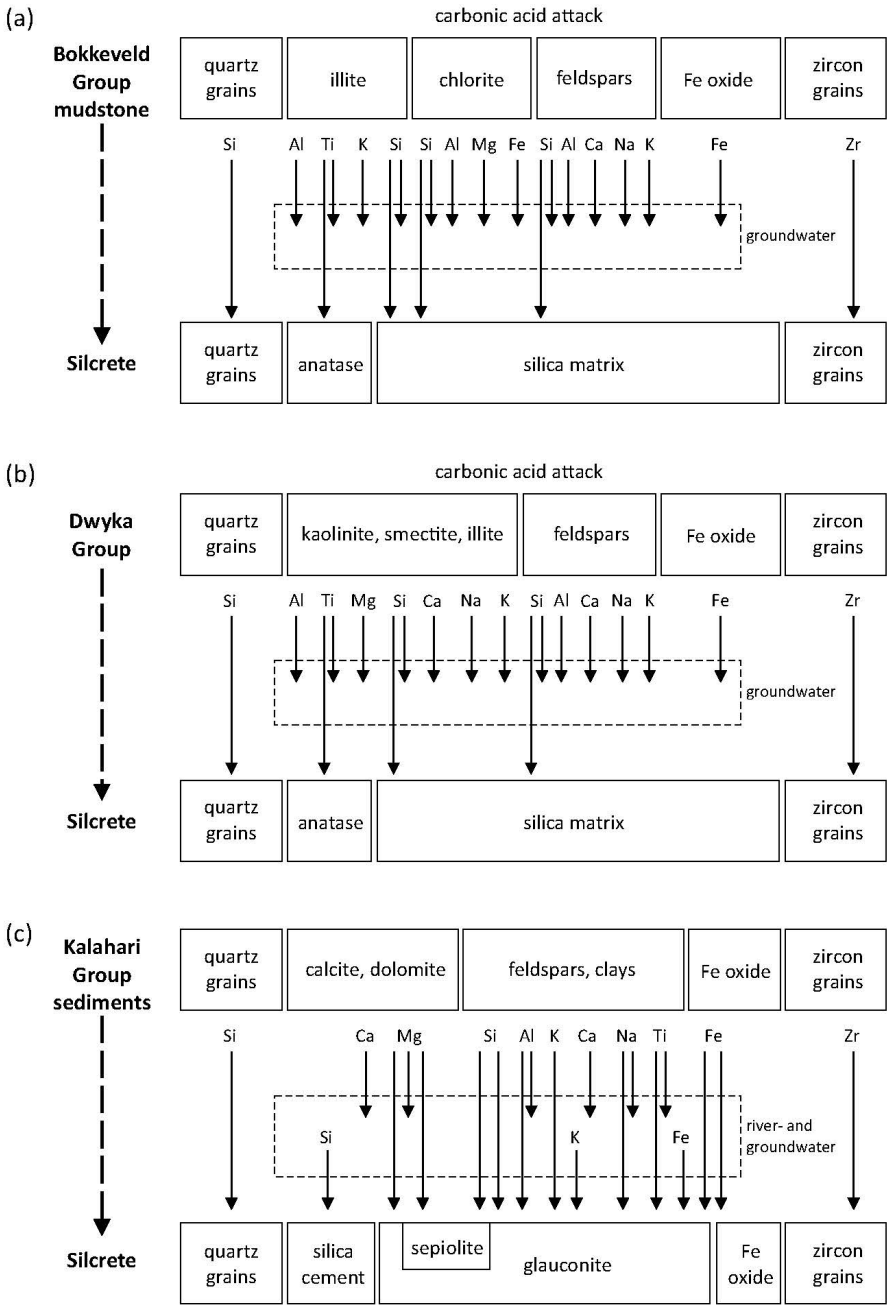

Figure 5
Schematic depiction of the changes in major element chemistry occurring during formation of silcretes in the Cape coastal zone (a, b) and Kalahari Desert (c).

The precipitation of silica within the regolith profile to form the Cape coastal silcretes could have been driven by evaporation within the soil profile (Webb and Golding, 1998; Lee and Gilkes, 2005), or by mixing of infiltrating silica-rich groundwater with deeper saline groundwater; the introduction of significant quantities of salt into a silica-rich solution can result in silica precipitation (Iler, 1979; Marshall and Warakomski, 1980).

The removal of most elements to very low levels during formation of the Cape silcretes (Figures 5a, b) implies an abundant source of infiltrating water, i.e. relatively high rainfall conditions. This is also indicated by the intensity of the weathering that destroyed the clays and feldspars, supporting Summerfield's (1983a) hypothesis that the Cape coastal silcretes formed under a relatively humid climate.

The isocon data indicate that the silica that formed the Cape silcretes was released during a period of intense weathering that led to the development of the thick weathered bedrock profiles found in the Cape coastal zone, i.e. silicification was contemporaneous with weathering. It is possible that the silica released into the groundwater at this time also silicified adjacent unconsolidated Cenozoic sediments, i.e. pedogenic and groundwater silicification in the Cape coastal zone could have been contemporaneous. If this is the case, then the intense weathering that formed the Cape silcretes must have occurred during the Cenozoic.

A potential candidate for the cause of this silicification event is the Palaeocene-Eocene Thermal Maximum (PETM), when there was a very rapid, massive addition of carbon dioxide into the atmosphere, increasing average global temperatures by approximately 6 °C (Kennett and Stott, 1991; Bowen et al., 2015). The increase in CO_2 levels in the atmosphere to 1700-2250 ppm (Panchuk et al., 2008; Zeebe et al., 2009) would have raised the carbonic acid levels of rainfall such that the acidity was ~2.5-3 times that of present rainfall, and the oceans rapidly acidified at the same time (Zachos et al., 2005). Intensified silicate weathering and pedogenesis was associated with the PETM, as shown by anomalously radiogenic Os-isotope compositions, significantly increased kaolinite abundances and anomalous silica-rich facies in sediments deposited at this time (Dypvik et al., 2011; Dickson et al., 2015; Chen et al., 2016); the latter apparently represent the burial of excess silica weathered off the continents during the PETM (Penman, 2016). The Eocene Climatic Optimum that followed the PETM was characterised by warm temperatures, high rainfall and deep weathering to high latitudes, and was accompanied by greatly increased silica levels in the oceans

(McGowran, 1989). Thus, the intense weathering that led to formation of the Cape silcretes could have occurred in the Eocene.

Since the weathering event that followed the Palaeocene-Eocene Thermal Maximum was world-wide, it would be expected that silcretes formed elsewhere at the same time. Therefore, silcrete formation in the Cape may have been synchronous with extensive silicification within the Eocene 'Polymorph Sandstone' in the southwest Congo Basin (cf. Tshibidi, 1986; Linol et al., 2015). Pedogenic silcretes similar to those in the Cape are known from central Australia (e.g. Wopfner, 1978; Thiry and Milnes, 1991; Webb and Golding, 1998), where some of them contain leaf impressions dated as Eocene (Greenwood et al., 1990; Greenwood, 1996; Hill et al., 2016), and from western Europe (e.g. Thiry and Simon-Coinçon, 1996; Thiry, 1999), where silcretes in the Paris Basin are regarded as Eocene in age on the basis of stratigraphy (Thiry, 1989). Thus it is possible that pedogenic silicification occurred around the world in the aftermath of the PETM.

Pedogenic silcretes are generally believed to have formed under acidic weathering conditions (e.g. Thiry, 1999; Nash and Ullyott, 2007; Taylor and Eggleton, 2017) to explain the dissolution of silicate minerals (clays and feldspars) and release of the silica required for silcrete formation. The source of the acidity has been variously ascribed to organic acids, oxidation of sulphide minerals and/or precipitation of ferric oxyhydroxides (Summerfield, 1983a; Nash and Ullyott, 2007; Taylor and Eggleton, 2017), but there is no evidence that any of these processes were active during formation of the Cape silcretes. Instead it is more likely that the acidity responsible for pedogenic silicification arrived as carbonic acid in the low pH rainfall that fell around the world during the PETM.

5. Kalahari Desert silcretes

5.1. Composition and mineralogy of host sediments in the Okavango system

The mineralogy of the surface sediments across the entire area covered by the Kalahari Group is dominated by quartz, with small amounts of fine-grained calcite and dolomite, clays (kaolinite, illite, smectite) and feldspars (plagioclase, microcline and K-feldspar) (McCarthy et al., 1991; McCarthy and Ellery, 1995; Chatupa and Direng, 2000; Huntsman-Mapila et al., 2005; Ringrose et al., 2014). The heavy minerals present vary according to the mineralogy of (often deeply) underlying bedrock: zircon, ilmenite, tourmaline, staurolite, kyanite, epidote, zoisite, andalusite, apatite, brookite, rutile, sillimanite, sphene, amphibole and garnet (Moore

and Dingle, 1998; Nuumbembe, 2016). In evaporitic pans, the near-surface sediments may contain halite and be covered by a surface crust of trona and thermonatrite (McCarthy et al., 1991).

Within the Okavango system, the chemical composition of the silcrete host sediments (Table 1) is dominated by SiO_2 (median 91 wt%), as expected given the preponderance of quartz sand, with minor amounts of other major elements, each of which is <1% except for Al_2O_3 and LOI (2 and 3 wt% respectively). Trace element concentrations are high for Ba (200 ppm) and Zr (100 ppm), moderate (10-35 ppm) for Sr, V, Co, Cr, Rb, Ce, Zn and Ta (in decreasing order of abundance), and low (<8 ppm) for all other trace elements.

The levels of CaO, MgO and LOI present (medians 0.6, 0.3 and 3 wt% respectively) are strongly correlated with each other and with Sr and U concentrations (r^2 = 0.94-0.95). All are present in calcite/dolomite; the affinity of carbonates for Sr and U has been well documented (e.g. Carlisle, 1983). The K_2O concentration (median 0.5 wt%) probably reflects the presence of illite and perhaps also K-feldspar.

The amounts of Fe_2O_3, TiO_2 and Al_2O_3 present in sediments of the Okavango system (median 0.8, 0.1 and 2 wt % respectively) are all well correlated (r^2 = 0.84-0.99). XRD and SEM studies by McCarthy and Ellery (1995) and Huntsman-Mapila et al. (2005) did not record any Fe- or Ti-rich heavy minerals in these sediments, and both suggested that the iron and titanium are associated with clays (mainly illite). It is likely the iron oxide coatings on the quartz grains, that impart the red-orange colour to much of the Kalahari sands, also play a role. Analyses of these coatings elsewhere in the Kalahari Desert showed that they contain Fe, Al, Ti and V (Vushe and Amutenya, 2019).

The levels of Fe_2O_3, TiO_2 and Al_2O_3 in sediments of the Okavango system are correlated (r^2 = 0.81-0.94) with a number of trace elements (V, Rb, Th, Ga, Y and REEs, except Tm and Lu), suggesting that the clays and/or iron oxide coatings have adsorbed these elements; iron oxides are known to strongly adsorb a variety of species (e.g. Dzombak and Morel, 1990).

The concentrations of Nb and Ta are strongly correlated with each other (r^2 = 0.82) but not with TiO_2. As noted above, the close similarity in ionic radius between Ti, Nb and Ta means that Ti-rich minerals can contain major amounts of Nb and Ta (Huy et al., 2012), so the lack of correlation between Nb-Ta and TiO_2 confirms the absence of Ti-rich heavy minerals in the Okavango sediments.

The presence of small amounts of zircon probably explains the level of Zr present (median 100 ppm). Zircon often contains Hf, but Hf concentrations also show a moderate correlation with Al-Ti-Fe and REEs, indicating that this element is present in the clays/iron oxide coatings as well as in zircon.

Although other heavy minerals have been recorded from the Kalahari Group, there is no evidence of these in the composition of the Okavango system sediments. For example, monazite, which is a phosphate mineral with high abundances of light rare earth elements (LREEs), has not been found and there is no correlation between P_2O_5 and LREE concentrations.

5.2. Composition and mineralogy of silcretes in the Okavango system

Duricrusts in the Kalahari sands include calcretes, silcretes and intergrade varieties between the two (Nash and Shaw, 1998; Nash et al., 2004); the discussion here is restricted to silcretes *sensu stricto* (i.e. >85 wt% SiO2; Summerfield, 1983a). The analytical data shows that the median composition of silcretes in the Okavango system (Table 1) is dominated by SiO_2 (median 94 wt%) with small amounts (<1.1 wt%) of Al_2O_3, K_2O, Fe_2O_3, MgO, CaO and TiO_2 (in decreasing order of abundance). Of the trace elements, Ba is the most abundant (~1000 ppm); there are high levels of Cr (~200 ppm), Sr and Zr (50 and 65 ppm respectively), low levels (3-20 ppm) of Rb, Ce, La, Nd and Y (in decreasing order of abundance), and very low levels (mostly <1 ppm) of other elements.

There is no significant difference between the median composition of silcretes within the Okavango system and the median composition of all Kalahari Desert silcretes (Table 1); although the Okavango system covers a limited geographical area, its sediments are derived from a range of bedrock, fluvial and aeolian sources and are therefore broadly representative of the Kalahari Group as a whole.

The mineralogy of the silcretes is dominated by quartz, both as inherited grains from the Kalahari sands and as cement filling the pore spaces between the grains. There may also be small amounts of calcite, effectively diluting the silica and resulting in negative correlations between Si and Ca (Nash et al., 2004).

The silcretes also commonly contain a dark green mineral, as both pan-lacustrine and drainage-line silcretes are often pale to dark green in colour (Boocock and van Straten, 1962; Nash et al., 2004); pan-lacustrine silcretes, in particular, may be strikingly green

(Summerfield, 1982). Thin section examination shows that the dark green mineral is present as rounded green-brown pellets 100-200 μm across as well as thin cement rims around quartz grains. This mineral was previously identified as glauconite by Summerfield (1982) and Du Plessis (1993), and XRD analysis during this study (Figure 6) confirmed the identification. Electron microprobe analyses of the green pellets from four different silcretes show that the glauconite contains, as expected, Si, Al, Fe, K and Mg, along with small amounts of Na (substituting for K), minor Ti and trace levels of Cr, Ni, Zn and V. The SiO_2 content is approximately double that typical of glauconite (~80% compared to 40-50%) because the glauconite pellets have been impregnated by silica during silcrete formation. If the microprobe analyses are adjusted to take this into account, the median composition of the glauconite is ~7% MgO, 10% Al_2O_3, 8% K_2O and 4.5% FeO.

Glauconite has a variable composition from K-poor, disordered glauconitic smectite to K-rich, ordered glauconitic mica; stages of development are defined by increasing K_2O content from ~2 wt.% (nascent) to >8 wt.% (highly evolved; Odin, 1988). The high K_2O content of the glauconite in Kalahari silcretes and the 10Å (8.75º 2θ) position of the 001 peak (Figure 6) are typical of micaceous glauconite, also indicated by the fibrous extinction pattern of the glauconite pellets under crossed polars in thin section. The levels of MgO in Kalahari silcretes are higher and total Fe lower than typical glauconite (1-5% and 10-25% respectively; Odin and Matter, 1981; Drits et al., 2010; Huggett and Cuadros, 2010).

Glauconite normally forms in shallowly buried, muddy, organic-rich marine sediments under sub-oxic conditions (Kelly and Webb, 1999; Kelly et al., 2001); the dark green colour reflects the fact that the Fe within glauconite is partly present as Fe^{2+} due to the reducing conditions during formation. However, the glauconite within the Kalahari silcretes formed in a terrestrial environment. Non-marine micaceous glauconite has been occasionally recorded from hypersaline lacustrine environments (Porrenga, 1968; Huggett and Cuadros, 2010), similar to the hypersaline pans where the darkest green Kalahari silcretes occur (Summerfield, 1982).

The presence of glauconite in the Kalahari silcretes explains the small amounts of Al_2O_3, K_2O, Fe_2O_3 and MgO present and the very strong correlation ($r^2 = 0.98$) of K and Al; other K-bearing minerals present in the Kalahari sands (K-feldspar and muscovite) were not detected by element mapping of silcrete thin sections. The Kalahari glauconite also contains

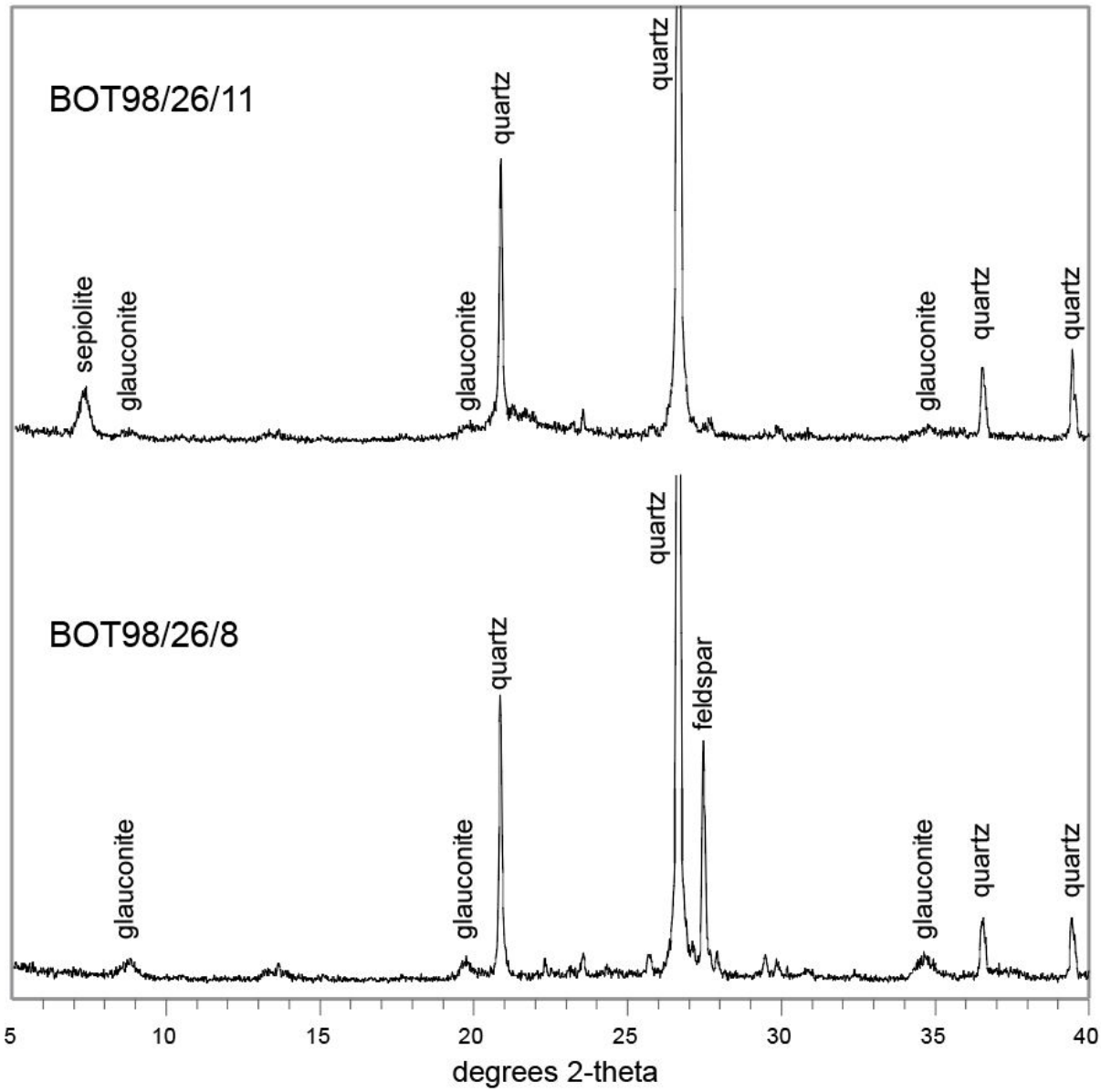

Figure 6
X-ray diffraction traces of two green Kalahari Desert silcrete samples from Tswaane, showing the presence of glauconite and sepiolite. See Figure 1 for location.

small amounts of Na (substituting for K) and minor Ti; this explains the strong correlation (r^2 = 0.84-0.86) of K with Na and Ti. The Rb in Kalahari glauconite is probably substituting for K, as these species are highly correlated (r^2 = 0.99) and micaceous glauconites typically contain 200-300 ppm Rb (Odin and Matter, 1981). Some trace elements in the Kalahari silcretes (Cs, Ga, Hf, Nb, Ta, Th, Zr, Cu, Pb and Zn) are strongly correlated with K (r^2 = 0.78-0.95), suggesting that these are also present in the glauconite.

Mg and Fe are not correlated with K within the Kalahari silcretes, despite the presence of all three elements in glauconite, because they are also present in other minerals. The hydrous

Mg silicate sepiolite was identified by XRD (Figure 6); this mineral is typically associated with silica precipitation in continental, often arid environments, including in the Kalahari Desert (Garrels and MacKenzie, 1967; Webb and Finlayson, 1987; Ringrose et al., 2009). It is likely that a small amount of Fe oxide/hydroxide is also present in some of the Kalahari silcretes, which contain higher levels of Fe than would be present just in glauconite.

The concentrations of Ba and Sr are very strongly correlated with S (r^2 = 0.87-0.92), implying that both are present as sulphates. This is consistent with the hypersaline conditions in the pans and groundwater (McCarthy and Metcalfe, 1990; McCarthy et al., 1991).

The REE concentrations are very strongly correlated (r^2 = 0.77-0.91) with each other (Ce, Dy, Er, Eu, Gd, Ho, La, Lu, Nd, Pr, Sm, Tb, Tm, Yb, Y) but not with any major elements or other trace elements. This suggests that they are present as a rare earth mineral, e.g. bastnasite, which is present in regolith-hosted rare earth deposits (Bao and Zhao, 2008), and/or xenotime, which can precipitate in sediments as minute grains or thin coatings on detrital zircon grains (McNaughton et al., 1999).

5.3. Formation of the silcretes in the Okavango system

The isocon comparison of the composition of sediments and silcretes in the Okavango system (Table 2; Figure 4) shows a substantial gain of SiO_2 (65%), Fe_2O_3 (30%) and K_2O (140%), minor loss of Al_2O_3, Na_2O and TiO_2 (10-20%), minor gain of MgO (20%) and substantial loss of CaO (70%). Among the trace elements, there are very large gains of Cr (>1000%) and Ba (600%), and substantial gains of Sr, Hf, Ga, U and Rb (>50%). Most REEs are almost stable (+-10%; Dy, Er, Eu, Gd, Nd, Pr, Sm, Y, Yb, La) but some show a loss (Ce, Tm) or gain (Ho, Tb). There are substantial losses (>50%) of only a few trace elements (Co, Nb, Ta and Zn).

To calculate the volume change during silicification using Equation 2, the density of the silcrete and parent material are required. The silcrete density is 2.64-2.66 g/cc, based on the porosity (<1%; Schmidt et al., 2017) and the content (3-4%) and density of glauconite (2.4-2.95 g/cc; Patchett et al., 1993); the density of unconsolidated Kalahari sands ranges from 1.4-1.8 g/cc (Schwartz et al., 1981; Pinard et al., 2014; Vushe and Amutenya, 2019). Inserting these values into Equation 2 along with the median Zr content of sediments and silcrete in the Okavango system (104 and 65 ppm respectively), the volume parent / volume silcrete ratio is 0.9-1.2 (Table 2), i.e. silicification is effectively isovolumetric. This is

consistent with the precipitation of silica within the pore spaces of the sands, which have 30-40% porosity (based on their density and composition).

The substantial addition of SiO_2 to the silcretes in the endorheic Okavango system (as cements and void fills; Nash and Hopkinson, 2004) is sourced primarily from water in the Okavango River, which has its headwaters in the Angolan highlands (Figure 1). The Okavango has an average annual discharge of ~1 x 10^{10} m^3 where it enters Botswana. The hydrological regime is dominated by low flows but with an annual flood pulse generated by rainfall over the headwaters in Angola; in exceptionally wet years, floodwaters may extend along the Boteti River (Figure 1). Substantially higher flows during the late Quaternary formed extensive palaeolakes linking the now discrete Ngami, Mababe and Makgadikgadi basins to the Okavango Delta (cf. Burrough et al., 2009). Because the system is endorheic, with internal drainage and no outflow, all the silica supplied during low flows and large floods is retained in the basin and is therefore available for silcrete formation.

The Okavango River presently delivers an estimated 360,000 tonnes of solutes to the Okavango Delta per year, ~50% of which can be dissolved silica, with concentrations up to 20 mg/L (McCarthy and Ellery, 1998; McCarthy, 2006); there is negligible solute input from rainfall (Milzow et al., 2009). Silica is removed biogenically as diatom frustules and phytoliths, which accumulate in stream and pan sediments in the Okavango Delta and its outflows (McCarthy and Ellery, 1995; Ringrose et al., 2014; Struyf et al., 2015).

The dissolved silica in the Okavango River was released by weathering of mafic silicates and feldspars in the Proterozoic granitoids and gneisses of the Angolan highlands, along with bicarbonate and cations including Ca. The composition of Okavango River water is characterised by a $mHCO_3^-$:mCa^{2+} ratio of > 2; evaporation of water with this ratio automatically produces an alkaline brine (following the Hardie-Eugster model; Drever, 1997). As a result, groundwater in parts of the Okavango system, particularly in areas where evapotranspiration is high such as the centres of islands in the Okavango Delta and pans in the distal Makgadikgadi Basin, often has a high pH (>10) and precipitates alkaline salts like trona (Na carbonate/bicarbonate; McCarthy and Metcalfe, 1990; Ringrose et al., 2009).

The high pH groundwater present in many parts of the Okavango system dissolves the diatom frustules and phytoliths in the upper layers of floodplain sediment (Ringrose et al., 2014; Struyf et al., 2015), because silica solubility increases greatly at pH > 9. As a result, this groundwater is silica-rich. Freshwater inflow to the Okavango Delta during seasonal

flooding (Milzow et al., 2009; Wolski et al., 2012) infiltrates into the groundwater and decreases its pH to circumneutral (5-6); the resulting drop in silica solubility causes the dissolved silica to precipitate within the pore spaces of the sandy sediments, forming silcrete. Strongly evaporative conditions following the cessation of flooding also help to drive silica precipitation (McCarthy et al., 1991; McCarthy and Ellery, 1995); evaporation rates are very high over the Okavango Delta (>2,000 mm yr^{-1}; McCarthy, 2006). Silcretes are found mainly in the distal part of the Okavango delta and its outflows, and this has been attributed to the progressive enrichment of silica in the surface water down the flow gradient due to evapotranspiration processes (McCarthy and Ellery, 1995; Shaw and Nash, 1998; Milzow et al., 2009).

The process of silicification within the Okavango system was accompanied by the dissolution of clay minerals within river, delta and pan sediments, because clay solubility increases significantly at alkaline pH (Carroll and Starkey, 1971). In addition, in the relatively organic-rich sediments of the Okavango Delta (McCarthy and Ellery, 1995), the ferric iron in the iron oxide coatings present on quartz grains would likely be reduced to soluble ferrous iron by the reducing conditions within the sediments, and removed. Reductive removal of the iron oxide sand coatings may be at least partly responsible for the white colour of most sands in the Okavango Delta itself, compared to the red-orange colour of adjacent wind-blown sands in areas immediately above the Okavango floodplain.

Many of the elements in the clays and iron oxide coatings were retained in silcrete through glauconite precipitation, which is widespread in Kalahari silcretes, although there was a loss of Al and Ti (Figure 5c). The gain of K in the silcretes was probably largely derived from the continuing input of K in the river water during seasonal or periodic flooding, released by weathering of K silicates (e.g. K-feldspar) in the gneisses and granitoids of the Angolan highlands. Dissolution of the small amounts of illite and K-feldspar present in the Kalahari sands would have also supplied K. The gain of Fe probably came from solution of the iron oxide coatings of sand grains in the sediments surrounding the silcrete.

The formation of glauconite was probably independent of silicification and more or less contemporaneous. The fact that glauconite pellets (where present) are silicified, as described previously, suggests that silicification may slightly postdate glauconite precipitation. Glauconite precipitation scavenges Rb (because this element substitutes readily for K) as well as Cr (Figure 4); glauconite can contain significant levels of Cr (Bitschene et al., 1992). The

gains of Hf and Ga during silcrete formation may also be due to incorporation into glauconite, as these trace elements in the silcretes are strongly correlated with K.

The loss of Ca during silicification indicates that the calcite originally present in the sediments has dissolved. The Sr released probably precipitated as a sulphate (as discussed above); the U released is retained but not by glauconite (there is no correlation between K and U in the silcretes).

The Cape silcretes contain anatase, but there is no evidence of anatase precipitation within the silcretes of the Okavango system; Ti is instead present within glauconite, as shown by the strong correlation between Ti and K. The losses of Nb and Ta during silicification confirm that no anatase has formed; in the Cape silcretes at least half of the Nb and Ta were retained because they were incorporated into anatase as it precipitated.

Overall there was no real loss or gain of REEs during silicification. This suggests that as these elements were released by dissolution of clays and iron oxide coatings, they were incorporated into a new mineral phase. As discussed above, this was probably a rare earth mineral. Rare earths are often mobile during weathering and can accumulate in the regolith profile, adsorbed to clays and/or as REE-hosting minerals, both residual (monazite) and neoformed like xenotime and bastnasite (McNaughton et al., 1999; Bao and Zhao, 2008).

The silicification process evident within the Okavango system (Figure 5c) is likely to be applicable to silcretes developed in Kalahari sands elsewhere in central southern Africa; these silcretes all have the same distinctive geochemical, mineralogical and textural features, reflecting the uniform silicification mechanism and parent materials. For example, glauconite is present at Tswaane on the Okwa River (Figure 6), a fossil feeder to the Makgadikgadi Basin but not connected to the Okavango River or its outflows. Granitoids, gneisses and basalts underlie much of the Kalahari Group, and weathering of the silicates in these rocks has influenced the composition of groundwater throughout the region, as shown by the alkaline pH (8.5-10.3) of groundwater within the Kalahari Group across Botswana (Batisani, 2012).

Overall, the major elements in the Kalahari silcretes were derived from the host sediments (Al, Mg, Ti, some of the Si, K, Fe), together with a considerable input from river water (K and Si) (Figure 5c). Additional Fe was probably derived from dissolution of the iron oxide coatings on sand grains in the sediments surrounding the silcrete. The bulk of the trace

elements probably also came from the Kalahari sands; the additional input of Cr and Ba may have come in river water.

There are no silcretes elsewhere in the world similar to the Kalahari Desert silcretes, particularly with respect to the association with alkaline groundwater and glauconite. Alkaline lakes occur in Death Valley, California (Garrels and MacKenzie, 1967), the lower Nile Valley in Egypt and the East African Rift (Schagerl and Renaut, 2016), but silcretes are unknown from these areas.

6. Comparison of Kalahari Desert and Cape silcretes

Compared to the Kalahari Desert silcretes, the Cape silcretes have considerably higher concentrations of TiO_2 (Table 1); in fact, there is virtually no overlap between the TiO_2 concentrations in the two silcrete types. For the other major elements, the Cape silcretes have lower levels of Al, Mg, Ca, K, Na and LOI, and for the trace elements, higher concentrations of most species apart from Ba, Cr, Sr and Rb, which are substantially greater in Kalahari silcretes (Table 1). This is despite the fact that silicification of the Cape silcretes resulted in almost complete loss of most major and trace elements (losses were lower for Si, Ti, Hf, Ta and Nb), whereas the Kalahari silcretes show a substantial gain of many elements (Si, Fe, K, Cr, Ba, Rb, Sr, Hf, Ga and U), with substantial losses (>50%) of only a few trace elements (Figures 5a, b, c). These differences are due to two factors: the composition of the host bedrock/sediments and the silicification process.

The Dwyka and Bokkeveld Group bedrock within which the Cape silcretes analysed here developed contains a high proportion of silicate minerals, particularly feldspars and clays, and as a result has much higher levels of TiO_2 and almost all trace elements than the Kalahari Group sands (Table 1). Even though the concentrations of these elements decreased substantially during silicification (Figure 4), sufficient were retained that Cape silcretes have greater amounts of TiO_2 and most trace elements. Geochemical evidence shows that formation of the Cape silcretes occurred during a period of intensive weathering that developed a thick regolith profile and caused a substantial reduction in volume (by a factor of 2.5-4), associated with the destruction of clays and other silicate minerals and almost complete loss of most major and trace elements. Much of the silica released from the silicate minerals was retained as a microcrystalline quartz matrix, forming the silcretes; most of the TiO_2 released from the silicates precipitated as microcrystalline anatase. As these elements

were released, they moved vertically downwards through the profile in groundwater over relatively short distances.

In contrast, formation of the Kalahari Desert silcretes involved accumulation rather than loss of elements; in particular there was a considerable input of K and Si, and probably also Cr and Ba, from river water (Figure 4). The precipitation of silica infilled the porosity in the sands, so silicification was close to isovolumetric. The major new mineral formed was glauconite, reflecting the suboxic groundwater conditions; there is no evidence of anatase precipitation. In the Okavango system, the additional elements in the river water were ultimately derived from weathering of basement rocks in the Angolan highlands; considerable long-distance transport has occurred. There were substantial losses during silicification of only a few elements (Figure 4). It is notable that Kalahari silcretes contain more Al than Cape silcretes even though their parent material has less (Table 1); this is probably because Al was retained by glauconite precipitation in the Kalahari silcretes, whilst no new Al-bearing mineral formed in the Cape silcretes. Silicification of the Kalahari silcretes was driven by evaporation and periodic input of floodwater under an arid to semi-arid climate; these processes are still occurring at the present day (McCarthy et al., 1991; McCarthy and Ellery, 1995; Ringrose et al., 2014). The crucial factor is that the evapotranspiration of groundwater in the Kalahari produces groundwater with a high pH that facilitates the mobility and precipitation of Si.

Cape coastal silcretes often cap dissected plateaus and overlie deeply weathered saprolite (Figure 2), because they formed by pedogenic silicification on palaeosurfaces. In contrast, the majority of Kalahari silcretes outcrop in or close to landscape depressions where the watertable is close to the surface, i.e. they are groundwater, pan-lacustrine or drainage-line silcretes.

In summary, the only real similarity between the Kalahari Desert and Cape silcretes is that they are both composed largely of silica. In almost all other aspects (non-silica geochemistry and mineralogy, process of silicification, occurrence in the landscape), they are totally different.

7. Implications for artefact sourcing studies

Analyses of silcretes from different parts of the Kalahari Desert and Cape coastal areas demonstrate small but significant differences in trace element composition (Nash et al.,

2013a; Nash et al., 2013b), and this has been used to identify likely source areas for artefacts from archaeological sites in the Kalahari Desert (Nash et al., 2013a; Nash et al., 2016). Provenance studies of artefacts rely on the distinctiveness of the source lithology (in this case its trace element composition); understanding the geological process that formed the artefact lithology is not necessarily important. However, a knowledge of how the southern African silcretes formed helps to understand the reliability of silcrete artefact sourcing, because differences in composition of the host lithology may not be reflected in differences in silcrete composition if relatively uniform geochemical changes during silcrete formation overprinted the variability in the host lithology. If this were the case, separate silcrete outcrops would be likely to have similar trace element compositions, meaning that artefact sourcing to a particular outcrop area is more difficult. On the other hand, if variability in the composition of the host lithology is faithfully reflected in the silcrete composition, then tracing artefacts to a single outcrop may be more probable.

The Kalahari silcretes, to a large extent, retain the trace element composition of the parent sands (Tables 1, 2), so any variations in composition of the sands, due to slight differences in their source, should be reflected in the composition of the silcrete. Nevertheless, there are significant gains and losses of a number of elements during silicification, and these could override the compositional differences of the parent material if they are uniform across the area (particularly if sourcing studies use ordination techniques that employ the entire dataset). So, to increase the likelihood of successful artefact sourcing, it should be based on the elements that show the least change during silicification, and specifically avoid those that show substantial gains (Cr, Ba, Rb, Sr, Hf, Ga and U). Those that suffered considerable loss (Co, Nb, Ta and Zn) could still be useful if their original relative proportions are approximately maintained.

For the Cape silcretes, only a small percentage of most trace elements was retained during silicification (Tables 1, 2), but nevertheless the anatase and iron oxide in the silcretes adsorbed a large suite of trace elements, albeit at low levels, and largely preserved the trace element signature of the bedrock. Therefore, any differences in the bedrock composition are maintained in the silcrete composition. There are substantial differences between the median compositions of the Dwyka and Bokkeveld Groups (Table 1), and it is likely that any smaller compositional differences between different outcrops of each unit, due to slight differences in the sediment supply, will be faithfully reflected in the silcrete composition. This means that

artefact sourcing of Cape silcretes to particular outcrops may be possible using trace elements.

8. Conclusions

Isocon studies of silcretes and their host materials in the Kalahari Desert and the Cape coastal zone have shown that, apart from the dominance of silica in their composition, they are very different. Silcretes in the Cape coastal zone are mostly pedogenic in origin, as shown by their columnar jointing and glaebular textures. Silcrete formation resulted from a period of intensive weathering of generally argillaceous bedrock that almost completely removed most major and trace elements, accompanied by a substantial decrease in volume (by a factor of 2.5-4). This process was independent of the bedrock on which the silcretes developed. Any silicate minerals present were destroyed; most of the elements released were moved vertically downwards in percolating groundwater, as shown by concave-upwards colloform structures. However, some of the silica was retained as a microcrystalline quartz matrix, and most of the Ti precipitated as anatase. The episode of intense weathering that led to formation of the Cape silcretes could have occurred in the Eocene, during and after the Palaeocene-Eocene Thermal Maximum. At this time elevated CO_2 levels in the atmosphere raised the acidity of rainfall and, together with relatively high temperatures, resulted in intensified silicate weathering around the globe. The pedogenic silcretes with a similar geochemistry and morphology that occur elsewhere the world could also have formed at this time; silcrete formation in the Cape may have been synchronous with Eocene silicification in the Congo Basin, central Australia and the Paris Basin.

Silcretes in the Kalahari Desert formed by approximately isovolumetric silicification of unconsolidated quartz sands, due to precipitation of silica in the pore spaces. This process involved substantial losses of only a few elements and accumulation of Si and K; the latter were incorporated into neoformed glauconite, which precipitated due to the suboxic groundwater conditions. There was no anatase precipitation, and the Kalahari silcretes have smaller amounts of TiO_2 and most trace elements than Cape silcretes due to the much lower concentrations of these species in the host sediments. The additional elements in the Kalahari silcretes were derived from weathering of basement rocks and supplied in river water; considerable long-distance transport of silica has occurred in the case of silcretes in the Okavango Delta and its outflows. Silicification of the Kalahari silcretes was driven by evaporation under an arid to semi-arid climate producing groundwater with a high pH that

facilitated the mobility and precipitation of Si. This process is still occurring but is not applicable to silcretes elsewhere in the world, which lack glauconite.

The results presented here are of significance for archaeological studies seeking to identify the raw material outcrops from which silcrete used in stone tool manufacture was sourced. Silcretes in the Cape coastal zone have been shown to largely retain the trace element signature of the underlying bedrock, which shows considerable geographic variation, so artefact sourcing to particular outcrops may be possible. For Kalahari silcretes, significant gains of some elements could override the compositional differences of the parent material, so to increase the likelihood of successful artefact sourcing it should be based on the elements that show the least change during silicification.

Acknowledgements

DJN acknowledges the University of Brighton for providing funding to support a sabbatical visit to Melbourne during which the original ideas for this paper were developed. Comments by Medard Thiry, Patrick Schmidt and an anonymous referee considerably improved this paper.

Data Availability Statement

All data used in this paper have been published previously, with data sources acknowledged in the text. A spreadsheet compilation of the dataset is available from the corresponding author on request.

Conflict of Interest

The authors have no conflict of interest to declare.

References

Baiyegunhi C, Nxantsiya Z, Pharoe K, Baiyegunhi TL, Mepaiyeda S. 2019. Petrographical and geophysical investigation of the Ecca Group between Fort Beaufort and Grahamstown, in the Eastern Cape Province, South Africa. *Open Geosciences* **11**: 313-326.

Bao ZW, Zhao ZH. 2008. Geochemistry of mineralization with exchangeable REY in the weathering crusts of granitic rocks in South China. *Ore Geology Reviews* **33**: 519-535.

Batisani N. 2012. Groundwater hydrochemistry evaluation in rural Botswana: a contribution to integrated water resources management. *Ethiopian Journal of Environmental Studies and Management* **5**: 521-528.

Bitschene PR, Holmes MA, Brezza J. 1992. Composition and Origin of Cr-Rich Glauconitic Sediments from the Southern Kerguelen Plateus (Site 748). In *Proceedings of the Ocean Drilling Program, Scientific Results 120*, Wise SW, Jr., Schlich R, Palmer Julson A, Aubry M-P, Berggren WA, Bitschene PR, Blackburn NA, Breza J, Coffin MF, Harwood DM, Heider F, Holmes MA, Howard WR, Inokuchi H, Kelts K, Lazarus DB, Mackensen A, Maruyama T, Munschy M, Pratson E, Quilty PG, Rack F, Salters VJM, Sevigny JH, Storey M, Takemura A, Watkins DK, Whitechurch H, Zachos JC (eds); 113-134.

Boocock C, van Straten OJ. 1962. Notes on the geology and hydrogeology of the Central Kalahari region, Bechuanaland Protectorate. *Transactions of the Geological Society of South Africa* **65**: 125-171.

Bosazza VL. 1939. The silcrete and clays of the Riversdale-Mossel Bay area. *Fulcrum, Johannesburg* **32**: 17-29.

Bothma S. 2015. *Geotechnical properties and foundation requirements for the satellite and lunar laser ranger at the Matjiesfontein Space Geodesy Observatory*. Master of Engineering thesis, Stellenbosch University: Stellenbosch.

Bowen GJ, Maibauer BJ, Kraus MJ, Rohl U, Westerhold T, Steimke A, Gingerich PD, Wing SL, Clyde WC. 2015. Two massive, rapid releases of carbon during the onset of the Palaeocene-Eocene thermal maximum. *Nature Geoscience* **8**: 44-47.

Burrough SL, Thomas DSG, Singarayer JS. 2009. Late Quaternary hydrological dynamics in the Middle Kalahari: forcing and feedbacks. *Earth-Science Reviews* **96**: 313-326.

Cahen L, Lepersonne J. 1952. *Équivalence entre le système du Kalahari du Congo belge et les Kalahari beds d'Afrique austral*. Mémoires de la Société Belge Géologique, Paléontologique, et Hydrologique, Série in-8, Sciences Géologiques 4: Tervuren, Belgium.

Carroll D, Starkey HC. 1971. Reactivity of clay minerals with acids and alkalies. *Clays and Clay Minerals* **19**: 321-333.

Chatupa JC, Direng BB. 2000. Distribution of trace and major elements in the -180 +75 μm and -75 μm fractions of the sandveld regolith in northwest Ngamiland, Botswana. *Journal of African Earth Sciences* **30**: 515-534.

Chen ZL, Ding ZL, Yang SL, Zhang CX, Wang X. 2016. Increased precipitation and weathering across the Paleocene-Eocene Thermal Maximum in central China. *Geochemistry Geophysics Geosystems* **17**: 2286-2297.

Dickson AJ, Cohen AS, Coe AL, Davies M, Shcherbinina EA, Gavrilov YO. 2015. Evidence for weathering and volcanism during the PETM from Arctic Ocean and Peri-Tethys osmium isotope records. *Palaeogeography Palaeoclimatology Palaeoecology* **438**: 300-307.

Drever JI. 1997. *The Geochemistry of Natural Waters: Surface and Groundwater Environments (Third Edition)*. Prentice Hall: Upper Saddle River, NJ.

Drits VA, Zviagina BB, McCarty DK, Salyn AL. 2010. Factors responsible for crystal-chemical variations in the solid solutions from illite to aluminoceladonite and from glauconite to celadonite. *American Mineralogist* **95**: 348-361.

Du Plessis PI. 1993. *The sedimentology of the Kalahari Group in four study areas in northern Botswana*. Master of Science thesis, University of Stellenbosch: Stellenbosch.

Dypvik H, Riber L, Burca F, Ruther D, Jargvoll D, Nagy J, Jochmann M. 2011. The Paleocene-Eocene thermal maximum (PETM) in Svalbard - clay mineral and geochemical signals. *Palaeogeography Palaeoclimatology Palaeoecology* **302**: 156-169.

Dzombak DA, Morel FMM. 1990. *Surface Complexation Modeling: Hydrous Ferric Oxide*. John Wiley: New York.

Eggleton RA, Taylor G. 2017. Titania in Australian massive silcretes. *Australian Journal of Earth Sciences* **64**: 1017-1026.

Fourie PF. 2010. *Provenance and paleotectonic setting of the Devonian Bokkeveld Group, Cape Supergroup, South Africa*. Magister Scientae thesis, University of Johannesburg: Johannesburg.

Frankel JJ. 1952. Silcrete near Albertinia, Cape Province. *South African Journal of Science* **49**: 173-182.

Frankel JJ, Kent LE. 1938. Grahamstown surface quartzites (silcretes). *Transactions of the Geological Society of South Africa* **15**: 1-42.

Garrels RM, MacKenzie FT. 1967. Origin of the chemical compositions of some springs and lakes. In *Equilibrium concepts in natural water systems. Advances in Chemistry Series 76*, Gould RF (ed). American Chemical Society: Washington; 222-242.

Grant JA. 2005. Isocon analysis: A brief review of the method and applications. *Physics and Chemistry of the Earth* **30**: 997-1004.

Greenwood DR. 1996. Eocene monsoon forests in central Australia? *Australian Systematic Botany* **9**: 95-112.

Greenwood DR, Callen RA, Alley NF. 1990. *The correlation and depositional environment of Tertiary strata based on macrofloras in the Southern Lake Eyre Basin*. South Australian Department of Mines and Energy, Report Book No. 90115: Adelaide.

Haddon IG, McCarthy TS. 2005. The Mesozoic-Cenozoic interior sag basins of Central Africa: The Late-Cretaceous-Cenozoic Kalahari and Okavango basins. *Journal of African Earth Sciences* **43**: 316-333.

Hill RS, Beer YK, Hill KE, Maciunas E, Tarran MA, Wainman CC. 2016. Evolution of the eucalypts - an interpretation from the macrofossil record. *Australian Journal of Botany* **64**: 600-608.

Huber H, Koeberl C, McDonald I, Reimold WU. 2001. Geochemistry and petrology of Witwatersrand and Dwyka diamictites from South Africa: Search for an extraterrestrial component. *Geochimica et Cosmochimica Acta* **65**: 2007-2016.

Huggett JM, Cuadros J. 2010. Glauconite formation in lacustrine/palaeosol sediments, Isle of Wight (Hampshire Basin), UK. *Clay Minerals* **45**: 35-49.

Huntsman-Mapila P, Kampunzu AB, Vink B, Ringrose S. 2005. Cryptic indicators of provenance from the geochemistry of the Okavango Delta sediments, Botswana. *Sedimentary Geology* **174**: 123-148.

Huy HA, Aradi B, Frauenheim T, Deak P. 2012. Comparison of Nb- and Ta-doping of anatase TiO_2 for transparent conductor applications. *Journal of Applied Physics* **112**: 016103. https://doi.org/10.1063/1.4733350.

Iler R. 1979. *The Chemistry of Silica: Solubility, Polymerization, Colloid and Surface Properties and Biochemistry*. John Wiley: New York.

Kampunzu AB, Ringrose S, Huntsman-Mapila P, Harris C, Vink BW, Matheson W. 2007. Origins and palaeo-environments of Kalahari duricrusts in the Moshaweng dry valleys (Botswana) as detected by major and trace element composition. *Journal of African Earth Sciences* **48**: 199-221.

Kanna M, Wongnawa S, Sherdshoopongse P, Boonsin P. 2005. Adsorption behaviour of some metal ions on hydrated amorphous titanium dioxide surface. *Songklanakarin Journal of Science and Technology* **27**: 1017-1026.

Kelly JC, Webb JA. 1999. The genesis of glaucony in the Oligo-Miocene Torquay Group, southeastern Australia: petrographic and geochemical evidence. *Sedimentary Geology* **125**: 99-114.

Kelly JC, Webb JA, Maas R. 2001. Isotopic constraints on the genesis and age of autochthonous glaucony in the Oligo-Miocene Torquay Group, south-eastern Australia. *Sedimentology* **48**: 325-338.

Kennett JP, Stott LD. 1991. Abrupt deep-sea warming, palaeoceanographic changes and benthic extinctions at the end of the Paleocene. *Nature* **353**: 225-229.

Lee SY, Gilkes RJ. 2005. Groundwater geochemistry and composition of hardpans in southwestern Australian regolith. *Geoderma* **126**: 59-84.

Linol B, de Villiers S, de Wit M. 2019. Accelerated contribution of the Paleo–Congo River to Global Seawater $^{87}Sr/^{86}Sr$ change following Eocene-Oligocene collapse of the African Surface. *Geochemistry, Geophysics, Geosystems* **20**: 1937-1953.

Linol B, de Wit MJ, Guillocheau F, de Wit MCJ, Anka Z, Colin J-P. 2015. Formation and collapse of the Kalahari duricrust ('African Surface') across the Congo Basin, with implications for changes in rates of Cenozoic offshore sedimentation. In *Geology and Resource Potential of the Congo Basin*, de Wit MJ, Guillocheau F, de Wit MCJ (eds). Springer-Verlag: Berlin; 193-210.

MacGregor AM. 1931. Geological notes on a circuit of the Great Makarikari Salt Pan, Bechuanaland Protectorate. *Transactions of the Geological Society of South Africa* **41**: 211-224.

Marker ME, McFarlane MJ, Wormald RJ. 2002. A laterite profile near Albertinia, Southern Cape, South Africa: its significance in the evolution of the African Surface. *South African Journal of Geology* **105**: 67-74.

Marshall WL, Warakomski JM. 1980. Amorphous silica solubilities 3. Activity-coefficient relations and predictions of solubility behavior in salt-solutions, 0-350-degrees-C. *Geochimica et Cosmochimica Acta* **44**: 925-931.

McCarthy TS. 2006. Groundwater in the wetlands of the Okavango Delta, Botswana, and its contribution to the structure and function of the ecosystem. *Journal of Hydrology* **320**: 264-282.

McCarthy TS, Ellery WN. 1995. Sedimentation on the distal reaches of the Okavango Fan, Botswana, and its bearing on calcrete and silcrete (ganister) formation. *Journal of Sedimentary Research Section A: Sedimentary Petrology and Processes* **65**: 77-90.

McCarthy TS, Ellery WN. 1998. The Okavango Delta. *Transactions of the Royal Society of South Africa* **53**: 157-182.

McCarthy TS, Metcalfe J. 1990. Chemical sedimentation in the semiarid environment of the Okavango Delta, Botswana. *Chemical Geology* **89**: 157-178.

McCarthy TS, McIver JR, Verhagen BT. 1991. Groundwater evolution, chemical sedimentation and carbonate brine formation on an island in the Okavango Delta swamp, Botswana. *Applied Geochemistry* **6**: 577-595.

McGowran B. 1989. Silica burp in the Eocene ocean. *Geology* **17**: 857-860.

McNaughton NJ, Rasmussen B, Fletcher IR. 1999. SHRIMP uranium-lead dating of diagenetic xenotime in siliciclastic sedimentary rocks. *Science* **285**: 78-80.

Milnes AR, Twidale CR. 1983. An overview of silicification in Cainozoic landscapes of arid central and southern Australia. *Australian Journal of Soil Research* **21**: 387-410.

Milzow C, Kgotlhang L, Bauer-Gottwein P, Meier P, Kinzelbach W. 2009. Regional review: the hydrology of the Okavango Delta, Botswana - processes, data and modelling. *Hydrogeology Journal* **17**: 1297-1328.

Moore AE, Dingle RV. 1998. Evidence for fluvial sediment transport of Kalahari sands in central Botswana. *South African Journal of Geology* **101**: 143-153.

Morton AC. 1984. Stability of detrital heavy minerals in tertiary sandstones from the North-Sea basin. *Clay Minerals* **19**: 287-308.

Mountain ED. 1952. The origin of silcrete. *South African Journal of Science* **48**: 201-204.

Nash DJ, Shaw PA. 1998. Silica and carbonate relationships in silcrete-calcrete intergrade duricrusts from the Kalahari of Botswana and Namibia. *Journal of African Earth Sciences* **27**: 11-25.

Nash DJ, Hopkinson L. 2004. A reconnaissance laser raman and fourier transform infrared survey of silcretes from the Kalahari Desert, Botswana. *Earth Surface Processes and Landforms* **29**: 1541-1558.

Nash DJ, Ullyott JS. 2007. Silcrete. In *Geochemical Sediments and Landscapes*, Nash DJ, McLaren SJ (eds). Blackwell: Oxford; 95-143.

Nash DJ, Thomas DSG, Shaw PA. 1994a. Siliceous duricrusts as palaeoclimatic indicators: evidence from the Kalahari Desert of Botswana. *Palaeogeography Palaeoclimatology Palaeoecology* **112**: 279-295.

Nash DJ, Shaw PA, Thomas DSG. 1994b. Duricrust development and valley evolution: process-landform links in the Kalahari. *Earth Surface Processes and Landforms* **19**: 299-317.

Nash DJ, Shaw PA, Ullyott JS. 1998. Drainage-line silcretes of the Middle Kalahari: an analogue for Cenozoic sarsen trains? *Proceedings of the Geologists' Association* **109**: 241-254.

Nash DJ, McLaren SJ, Webb JA. 2004. Petrology, geochemistry and environmental significance of silcrete-calcrete intergrade duricrusts at Kang Pan and Tswaane, Central Kalahari, Botswana. *Earth Surface Processes and Landforms* **29**: 1559-1586.

Nash DJ, Coulson S, Staurset S, Ullyott JS, Babutsi M, Hopkinson L, Smith MP. 2013a. Provenancing of silcrete raw materials indicates long-distance transport to Tsodilo Hills, Botswana, during the Middle Stone Age. *Journal of Human Evolution* **64**: 280-288.

Nash DJ, Coulson S, Staurset S, Smith MP, Ullyott JS. 2013b. Provenancing silcrete in the Cape coastal zone: implications for Middle Stone Age research in South Africa. *Journal of Human Evolution* **65**: 682-688.

Nash DJ, Coulson S, Staurset S, Ullyott JS, Babutsi M, Smith MP. 2016. Going the distance: Mapping mobility in the Kalahari Desert during the Middle Stone Age through multi-site geochemical provenancing of silcrete artefacts. *Journal of Human Evolution* **96**: 113-133.

Nuumbembe WP. 2016. *Analysis of the Namib and Kalahari dune sand deposits in Namibia and their application in potassium silicate synthesis*. Master of Science thesis, University of Namibia: Windhoek.

Odin GS. 1988. *Green Marine Clays: Oolitic Ironstone Facies, Verdine Facies, Glaucony Facies and Celadonite-Bearing Facies - A Comparative Study*. Elsevier: Amsterdam.

Odin GS, Matter A. 1981. De glauconiarum origine. *Sedimentology* **28**: 611-641.

Panchuk K, Ridgwell A, Kump LR. 2008. Sedimentary response to Paleocene-Eocene Thermal Maximum carbon release: A model-data comparison. *Geology* **36**: 315-318.

Patchett JG, Wiley R, El Bahr M. 1993. *Modeling the effects of glauconite on some openhole logs from the Lower Senonian in Egypt*. Society of Petrophysicists and Well-Log Analysts 34th Annual Logging Symposium, 13-16 June: Calgary, Alberta.

Penman DE. 2016. Silicate weathering and North Atlantic silica burial during the Paleocene-Eocene Thermal Maximum. *Geology* **44**: 731-734.

Pettijohn FJ. 1941. Persistence of heavy minerals and geological age. *Journal of Geology* **49**: 610-625.

Pinard MI, Paige-Green P, Mukura K, Bofinger H, Motswagole KJ, Netterberg F. 2014. *Guide for the Use of Sand in Road Construction in the SADC Region*. Association of Southern African National Roads Agencies: Pretoria.

Porrenga DH. 1968. Non-marine glauconitic illite in the Lower Oligocene of Aardebrug, Belgium. *Clay Minerals* **7**: 421-430.

Reimold WU, von Brunn V, Koeberl C. 1997. Are diamictites impact ejecta? No supporting evidence from South African Dwyka Group diamictite. *Journal of Geology* **105**: 517-530.

Ringrose S, Huntsman-Mapila P, Basira Kampunzu A, Downey W, Coetzee S, Vink B, Matheson W, Vanderpost C. 2005. Sedimentological and geochemical evidence for palaeo-environmental change in the Makgadikgadi subbasin, in relation to the MOZ rift depression, Botswana. *Palaeogeography, Palaeoclimatology, Palaeoecology* **217**: 265-287.

Ringrose S, Harris C, Huntsman-Mapila P, Vink BW, Diskins S, Vanderpost C, Matheson W. 2009. Origins of strandline duricrusts around the Makgadikgadi Pans (Botswana Kalahari) as deduced from their chemical and isotope composition. *Sedimentary Geology* **219**: 262-279.

Ringrose S, Cassidy L, Diskin S, Coetzee S, Matheson W, Mackay AW, Harris C. 2014. Diagenetic transformations and silcrete-calcrete intergrade duricrust formation in palaeo-estuary sediments. *Earth Surface Processes and Landforms* **39**: 1167-1187.

Roberts DL. 2003. *Age, Genesis and Significance of South African Coastal Belt Silcretes*. Memoir 95, Council for Geoscience: Pretoria.

Schagerl M, Renaut RW. 2016. Dipping into the soda lakes of East Africa. In *Soda Lakes of East Africa*, Schagerl M (ed). Springer International; 3-24.

Schmidt P, Nash DJ, Coulson S, Göden MB, Awcock GJ. 2017. Heat treatment as a universal technical solution for silcrete use? A comparison between silcrete from the Western Cape (South Africa) and the Kalahari (Botswana). *PLoS ONE* **12**: e0181586. https://doi.org/10.1371/journal.pone.0181586.

Schwartz K, Yates JRC, Tromp BE. 1981. In situ compaction of aeolian Kalahari Sand. In *Proceedings of the 10th International Conference on Soil Mechanics and Foundation Engineering (Stockholm)*. International Society for Soil Mechanics and Geotechnical Engineering; 773-776.

Shaw PA, de Vries JJ. 1988. Duricrust, groundwater and valley development in the Kalahari of southeast Botswana. *Journal of Arid Environments* **14**: 245-254.

Shaw PA, Nash DJ. 1998. Dual mechanisms for the formation of fluvial silcretes in the distal reaches of the Okavango Delta Fan, Botswana. *Earth Surface Processes and Landforms* **23**: 705-714.

Shaw PA, Cooke HJ, Perry CC. 1990. Microbialitic silcretes in highly alkaline environments: some observations from Sua Pan, Botswana. *South African Journal of Geology* **93**: 803-808.

Struyf E, Mosimane K, Van Pelt D, Murray-Hudson M, Meire P, Frings P, Wolski P, Schaller J, Gondwe MJ, Schoelynck J, Conley DJ. 2015. The Role of Vegetation in the Okavango Delta Silica Sink. *Wetlands* **35**: 171-181.

Summerfield MA. 1981. *The nature and occurrence of silcrete, southern Cape Province, South Africa*. School of Geography Research Paper 28, University of Oxford: Oxford.

Summerfield MA. 1982. Distribution, nature and genesis of silcrete in arid and semi-arid southern Africa. *Catena* **Supplement 1**: 37-65.

Summerfield MA. 1983a. Silcrete as a paleoclimatic indicator - evidence from southern Africa. *Palaeogeography Palaeoclimatology Palaeoecology* **41**: 65-79.

Summerfield MA. 1983b. Geochemistry of weathering profile silcretes, southern Cape Province, South Africa. In *Residual Deposits: Surface Related Weathering Processes and Materials*, Wilson RCL (ed). Special Publication 11, Geological Society: London; 167-178.

Summerfield MA. 1983c. Petrography and diagenesis of silcrete from the Kalahari Basin and Cape coastal zone, southern Africa. *Journal of Sedimentary Petrology* **53**: 895-909.

Summerfield MA. 1984. Isovolumetric weathering and silcrete formation, southern Cape Province, South Africa. *Earth Surface Processes and Landforms* **9**: 135-141.

Taylor G, Eggleton RA. 2017. Silcrete: an Australian perspective. *Australian Journal of Earth Sciences* **64**: 987-1016.

Thiry M. 1989. Geochemical evolution and paleoenvironments of the Eocene continental deposits in the Paris Basin. *Palaeogeography Palaeoclimatology Palaeoecology* **70**: 153-163.

Thiry M. 1999. Diversity of continental silicification features: examples from the Cenozoic deposits in the Paris Basin and neighbouring basement. In *Palaeoweathering, Palaeosurfaces and Related Continental Deposits*, Thiry M, Simon-Coinçon R (eds).

International Association of Sedimentologists, Special Publication No 27. Blackwell Science: Oxford; 87-127.

Thiry M, Simon-Coinçon R. 1996. Tertiary palaeoweatherings and silcretes in the southern Paris Basin. *Catena* **26**: 1-26.

Thiry M, Milnes AR. 1991. Pedogenic and groundwater silcretes at Stuart Creek opal field, South Australia. *Journal of Sedimentary Petrology* **61**: 111-127.

Thiry M, Milnes A. 2017. Silcretes: Insights into the occurrences and formation of materials sourced for stone tool making. *Journal of Archaeological Science-Reports* **15**: 500-513.

Thomas DSG, Shaw PA. 1991. *The Kalahari Environment*. Cambridge University Press: Cambridge.

Thornber MR. 1992. The chemical mobility and transport of elements in the weathering environment. In *Regolith Exploration Geochemistry in Tropical and Subtropical Terrains*, Butt CRM, Zeegers H (eds). Handbook of Exploration Geochemistry 4. Elsevier: Amsterdam; 79-96.

Tshibidi NyB. 1986. Le ciment siliceux dans les grès polymorphes du plateau des Biano (Shaba-Zaire) provient en partie de la silicification d'une matrice carbonatée. *Annales de la Société géologique de Belgique* **109**: 579-585.

Twidale CR, Hutton JT. 1986. Silcrete as a climatic indicator: Discussion. *Palaeogeography, Palaeoclimatology, Palaeoecology* **52**: 351-356.

Ullyott JS, Nash DJ. 2016. Distinguishing pedogenic and non-pedogenic silcretes in the landscape and geological record. *Proceedings of the Geologists' Association* **127**: 311-319.

Ullyott JS, Nash DJ, Shaw PA. 1998. Recent advances in silcrete research and their implications for the origin and palaeoenvironmental significance of sarsens. *Proceedings of the Geologists' Association* **109**: 255-270.

Veatch AC. 1935. *Evolution of the Congo Basin*. Geological Society of America, Memoir 3: Washington DC.

Vushe A, Amutenya M. 2019. Investigating nitrate retention capacity, elementary and mineral composition of Kalahari sandy soils at Mashare farm in Namibia, Okavango river basin. *Scientific African* **6**: e00193. https://doi.org/10.1016/j.sciaf.2019.e00193.

Wang X, Griffin WL, Chen J. 2010. Hf contents and Zr/Hf ratios in granitic zircons. *Geochemical Journal* **44**: 65-72.

Watts SH. 1978. A petrographic study of silcrete from inland Australia. *Journal of Sedimentary Petrology* **48**: 987-994.

Webb JA, Finlayson BL. 1987. Incorporation of Al, Mg, and water in opal-a - evidence from speleothems. *American Mineralogist* **72**: 1204-1210.

Webb JA, Golding SD. 1998. Geochemical mass-balance and oxygen-isotope constrains on silcrete formation and its paleoclimatic implications in Southern Australia. *Journal of Sedimentary Research* **68**: 981-993.

Wolski P, Todd MC, Murray-Hudson MA, Tadross M. 2012. Multi-decadal oscillations in the hydro-climate of the Okavango River system during the past and under a changing climate. *Journal of Hydrology* **475**: 294-305.

Wopfner H. 1978. Silcretes of northern South Australia and adjacent regions. In *Silcrete in Australia*, Langford-Smith T (ed). University of New England Press: Armidale; 93-141.

Young RW. 1985. Silcrete distribution in eastern Australia. *Zeitschrift für Geomorphologie* **29**: 21-36.

Zachos JC, Rohl U, Schellenberg SA, Sluijs A, Hodell DA, Kelly DC, Thomas E, Nicolo M, Raffi I, Lourens LJ, McCarren H, Kroon D. 2005. Rapid acidification of the ocean during the Paleocene-Eocene thermal maximum. *Science* **308**: 1611-1615.

Zeebe RE, Zachos JC, Dickens GR. 2009. Carbon dioxide forcing alone insufficient to explain Palaeocene-Eocene Thermal Maximum warming. *Nature Geoscience* **2**: 576-580.

Median composition		SiO_2	Al_2O_3	Fe_2O_3	CaO	MgO	Na_2O	K_2O	TiO_2	MnO	P_2O_5	SO_3	LOI	Ba	Ce	Cr	Cs	Dy	Er	Eu	Ga	Gd	Hf	Ho	La	Lu	Nb	Nd	Pr	Rb
Dwyka Gp	bedrock	67.9	13.1	5.25	1.96	2.46	2.73	2.51	0.71	0.11	0.16	0.49	2.44	847	75.4	127	1.62			1.32	46	5.8	5.71		37.3	0.41	14	34.7		96.8
	silcrete	93.05	0.79	2.05	0.02	0.02	0.01	0.02	1.73	0.00	0.02	0.02	0.46	197.5	11.8	80	0.07	1.92	1.56	0.2	8.2	0.93	21	0.42	6.6	0.38	25	4	1.23	0.9
Bokkeveld Gp	bedrock	61.2	17.7	6.76	0.1	1.61	0.61	3.45	0.95	0.03	0.14		5.69	695.1	92	117.9	9				24.9		9.5		45		19.7			162.4
	silcrete	95.8	0.52	0.60	0.04	0.02	0.05	0.02	1.72	0.01	0.01		0.75	163.5	17	40	0.07	2.25	1.74	0.27	3.8	1.41	13.3	0.51	11.1	0.35	30.7	6.2	1.81	1.1
Okavango	sediments	90.6	1.84	0.745	0.62	0.29	0.15	0.48	0.12	0.01	0.01		2.79	204	16	22	0.65	0.9	0.6	0.3	1	1.1	1	0.1	8	0	6	6.5	1.8	19
	silcrete	94.3	1.06	0.71	0.11	0.16	0.08	0.76	0.055	0.01	0.01	0.02		939.5	8.15	210	0.35	0.64	0.38	0.175	1.2	0.74	1.9	0.125	6.55	0.06	0.95	4.7	1.32	19.5
Kal. overall	silcrete	93.4	1.13	0.69	0.13	0.35	0.08	0.53	0.07	0.01	0.01	0.02	2.55	1137.5	7.6	210	0.31	0.58	0.35	0.155	1.1	0.7	1.45	0.115	6.3	0.05	0.9	4.65	1.24	13.6
Cape overall	silcrete	95.4	0.53	0.85	0.02	0.03	0.04	0.02	1.71	0.005	0.03	0.01	0.72	177.8	13.1	50	0.07	2.01	1.68	0.23	5.1	1.24	14.4	0.47	8.1	0.35	27.0	4.85	1.33	1.05

Median composition		Sc	Sm	Sn	Sr	Ta	Tb	Th	Tl	Tm	U	V	W	Y	Yb	Zr	As	Bi	Hg	Sb	Se	Te	Ag	Cd	Co	Cu	Mo	Ni	Pb	Zn
Dwyka Gp	bedrock	13.1	6.31		145	0.9	0.84	12.9		0.38	2.36	103	1.21	28	2.82	197	2.69			0.29	0.33				14.9	9		51		77
	silcrete		0.82	4	20	2	0.24	11		0.27	2.88	94	3	12.2	2.11	741	3.7	0.17	0.059	0.25	1.2	0.02			1	12	3	1	24	3
Bokkeveld Gp	bedrock	18.7			85.4	1.4		15.9			2.9	112.6		34.7		188.2									13.1	21.3		25.7	25.3	77.2
	silcrete		1.31	5	21.8	2.5	0.31	6.88	0	0.29	2.87	49	4	15.2	2.13	499	1.3	0.09	0.042	0.11	0	0	0	0	2	15	4	2	13	2
Okavango	sediments	5	1.2		35.2	11	0.1	2		0.1	1	35		6	0.6	104									33	5		4	4.5	15
	silcrete		0.9	0	46.8	0.1	0.11	0.875	0	0.05	1.345	12	1	3.65	0.35	69.5	1.05	0.02	0	0.07	0	0	0	0	1	2	0	3	3	0
Kal. overall	silcrete		0.84	0	51.7	0.1	0.095	0.82	0	0.05	1.6	19	1	3.35	0.32	54	1.05	0.01	0	0.07	0	0	0	0	1.5	3	0	3.5	3	1
Cape overall	silcrete		1.07	5	20.95	2.15	0.28	8.25	0	0.29	2.84	56.5	3	14.0	2.06	521.5	2.05	0.12	0.049	0.17	0.3	0.01	0	0	1	13.5	3	2	17.5	2

Table 1
Median analyses of Cape and Kalahari silcrete and associated bedrock/sediments; major elements as wt% and trace elements as ppm; LOI = loss on ignition. Overall medians include all available silcrete analyses for each region, not just Cape silcretes overlying Dwyka/Bokkeveld Group bedrock or Kalahari silcretes in the Okavango Delta.

A	B	C	D	E	F	G	H	I	J	K	L	M	N	O	P	Q	R	S	T	U	V	W	X	Y	Z	AA
			SiO_2	Al_2O_3	Fe_2O_3	CaO	MgO	Na_2O	K_2O	TiO_2	MnO	P_2O_5	LOI	Ba	Ce	Cr	Cs	Dy	Er	Eu	Ga	Gd	Hf	Ho	La	Lu
% gain/loss	$Zr_{parent}/Zr_{silcrete}$	$V_{parent}/V_{silcrete}$																								
Dwyka Gp	0.27	3.5 - 3.9	-63.6	-98.4	-89.6	-99.7	-99.8	-99.9	-99.8	-35.4	-100.0	-96.7	-95.0	-93.8	-95.8	-83.3	-98.9			-96.0	-95.3	-95.7	-2.2		-95.3	-75.4
Dwyka Gp*	0.27	3.5 - 3.9	-63.0	-98.4	-83.0	-82.4	-96.5	-100.0	-81.2	-57.7	-100.0		-97.8													
Bokkeveld Gp	0.38	2.5 - 2.8	-41.0	-98.9	-96.7	-84.9	-99.5	-96.9	-99.8	-31.7	-87.4	-97.3	-95.1	-91.1	-93.0	-87.2	-99.7				-94.2		-47.2		-90.7	
Okavango	1.50	1.0 - 1.3	55.7	-14.2	42.6	-73.5	-16.0	-20.2	135.4	-31.4	50.0	50.0		589.2	-23.8	1328	-19.4	6.4	-5.2	-12.7	79.6	0.7	184.3	87.1	22.5	

			Nb	Nd	Pr	Rb	Sm	Sr	Ta	Tb	Th	Tm	U	V	W	Y	Yb	Zr	As	Sb	Se	Co	Cu	Ni	Pb	Zn
% gain/loss																										
Dwyka Gp			-52.5	-96.9		-99.8	-96.5	-96.3	-40.9	-92.4	-77.3	-81.1	-67.6	-75.7	-34.1	-88.4	-80.1	0.0	-63.4	-77.1	-3.3	-98.2	-64.6	-99.5		-99.0
Dwyka Gp*																										
Bokkeveld Gp			-41.2			-99.7		-90.4	-32.7		-83.7		-62.7	-83.6		-83.5		0.0				-94.2	-73.4	-97.1	-80.6	-99.0
Okavango			-76.3	8.2	9.7	53.2	12.2	99.0	-98.6	64.6	-34.5	-25.2	101.3	-48.7		-9.0	-14	0.0				-95.5	-40.1	12.2	-0.24	-100.0

Table 2
Percentage gain/loss for each element calculated from the isocon analysis; LOI = loss on ignition. See text for details. Missing values indicate that the silcrete and/or host material analyses lacked this element.